frontiers in Physics

REVIEW
published: 13 June 2019
doi: 10.3389/fphy.2019.00086

Neutrinoless Double Beta Decay Experiments With TeO_2 Low-Temperature Detectors

*Chiara Brofferio [1,2], Oliviero Cremonesi [2] and Stefano Dell'Oro [3]**

[1] Dipartimento di Fisica, Università di Milano-Bicocca, Milan, Italy, [2] Istituto Nazionale di Fisica Nucleare (INFN), Sezione di Milano-Bicocca, Milan, Italy, [3] Center for Neutrino Physics, Virginia Polytechnic Institute and State University, Blacksburg, VA, United States

Neutrinoless double beta decay ($0\nu\beta\beta$) is a powerful tool to investigate Lepton Number Violation (LNV), and the only practical way to assess the nature of the neutrinos. It can therefore provide unique information about the Physics Beyond the Standard Model. If observed, $0\nu\beta\beta$ would unambiguously demonstrate that neutrinos are Majorana particles and would provide a precise measurement of their mass. Among the many experimental techniques used in the search for this rare process, low-temperature detectors represent one of the most promising choices: they show an excellent energy resolution and can scale to very large masses. In this work, we review the most relevant experiments based on TeO_2 bolometers that have been developed and taking data at the Laboratori Nazionali del Gran Sasso (LNGS), Italy, since the early 90's. This 30-years-old effort has led to the design and construction of the CUORE detector, currently taking data at LNGS. The use of low-temperature detectors allows to study the $0\nu\beta\beta$ of ^{130}Te on both ground and excited states, and to explore different decay mechanisms ("standard" light neutrino exchange, Majoron emission, …). At the same time, the investigation of other rare nuclear physics processes is also possible, such as the two-neutrino double beta decay of ^{130}Te as well as the rare decays (^{120}Te and ^{123}Te). Next generation bolometric experiments anticipate top leading sensitivities. The corresponding challenges in the development of ton-scale, low background detectors are highlighted.

Keywords: neutrinoless double beta decay, Majorana fermions, bolometers, low-background, CUORE

OPEN ACCESS

Edited by:
Alexander S. Barabash, Institute for Theoretical and Experimental Physics, Russia

Reviewed by:
Volodymyr I. Tretyak, Institute for Nuclear Research, National Academy of Sciences of Ukraine (NAN Ukraine), Ukraine
Steven Ray Elliott, Los Alamos National Laboratory (DOE), United States

****Correspondence:***
Stefano Dell'Oro
sdelloro@vt.edu

Specialty section:
This article was submitted to High-Energy and Astroparticle Physics, a section of the journal Frontiers in Physics

Received: *01 March 2019*
Accepted: *17 May 2019*
Published: *13 June 2019*

Citation:
Brofferio C, Cremonesi O and Dell'Oro S (2019) Neutrinoless Double Beta Decay Experiments With TeO_2 Low-Temperature Detectors. Front. Phys. 7:86. doi: 10.3389/fphy.2019.00086

1. INTRODUCTION

Neutrinoless double beta decay ($0\nu\beta\beta$) [1] is a hypothesized nuclear transition, forbidden in the framework of the Standard Model (SM). In this extremely rare process, a pair of free electrons is created in the transformation from a nucleus (A, Z) into its daughter $(A, Z+2)$, namely:

$$(A, Z) \rightarrow (A, Z+2) + 2e^{-}. \quad (1)$$

Similar transitions could proceed through the emission of a pair of positrons, double electron capture (EC), or EC plus single emission of a positron, with the nucleus changing from (A, Z) to $(A, Z-2)$. All these variations are equally interesting when discussing of new Physics, since they all manifest a non-conservation of the number of leptons (see section 6). The observation of one of these processes would therefore demonstrate that the lepton number is not a symmetry of Nature. Such a scenario would open the way to a possible explanation of the Baryon Asymmetry of the

Universe via Leptogenesis, thus solving another big mystery of Nature [2]. $0\nu\beta\beta$ is a fundamental tool to study neutrinos, since it can exist only if they are Majorana particles (the transition could not take place otherwise) and it can provide us with precious information on the neutrino absolute mass scale and ordering, a major clue nowadays.

The experimental search for $0\nu\beta\beta$ is based on the detection and exact measurement of the sum of the kinetic energies of the two emitted electrons or positrons. In fact, since the energy of the recoiling nucleus is negligible, the sum of the two leptons' kinetic energy must be equal to the Q-value of the transition, $Q_{\beta\beta}$, and it should appear in the energy spectrum as a monochromatic peak.

The experimental parameter extracted from the data is the half-life of the decay of the isotope under study, $t^{0\nu}_{1/2}$. In the fortunate case of a $0\nu\beta\beta$ peak showing up in the energy spectrum, this parameter can be deduced from the radioactive decay law:

$$t^{0\nu}_{1/2} = \ln 2 \; T \, \varepsilon \; \frac{N_{\beta\beta}}{N_{\text{peak}}} \tag{2}$$

where T is the measuring time, ε is the detection efficiency, $N_{\beta\beta}$ is the number of $\beta\beta$-decaying nuclei under observation, and N_{peak} is the number of counts at the peak. If no peak is detected, the sensitivity of a given $0\nu\beta\beta$ experiment, $S^{0\nu}_{1/2}$, is usually defined as the minimum half-life compatible with the background fluctuations n_B at a given confidence level. In the assumption that the background counts scale linearly with the mass of the detector[1], we have at 1σ:

$$n_B = \sqrt{M \; T \; B \; \Delta} \tag{3}$$

where M is the detector mass, B is the background level per unit mass, energy, and time in the region of interest (ROI) around $Q_{\beta\beta}$ and Δ is the FWHM energy resolution (used conventionally as the region over which to integrate B). Therefore, starting from Equation (2), it is easy to obtain the expression:

$$S^{0\nu}_{1/2} = \ln 2 \; \varepsilon \; \frac{1}{n_\sigma} \; \frac{x \, \eta \, N_A}{\mathscr{M}_A} \sqrt{\frac{M \; T}{B \; \Delta}} \tag{4}$$

where x is the stoichiometric multiplicity of the element containing the $\beta\beta$ candidate, η is the $\beta\beta$ candidate isotopic abundance, N_A is the Avogadro number, $\mathscr{M}_A$ is the compound molecular mass and n_σ is the number of sigmas corresponding to the requested C. L. . Despite its simplicity, this expression clearly shows the role of the basic experimental parameters: improving one or more of these quantities will enhance the sensitivity on $t^{0\nu}_{1/2}$, and this is what drives the experimental decisions and efforts in the search for $0\nu\beta\beta$.

Equation (4) isn't valid anymore if the background level is so low that the expected number of background events in the ROI collected during the experiment is nearly zero. This is the so called "zero background" experimental condition. The transition between the two regimes takes place when the expected number of counts is of the order of unity:

$$M \; T \; B \; \Delta = \mathcal{O}(1). \tag{5}$$

In this case, we replace the background term in Equation (3) with n_L, i.e., the maximum number of counts compatible with zero at a given C. L. (in the assumption of Poisson statistics). The new expression for the sensitivity thus becomes:

$$S^{0\nu}_{1/2,\,0\text{bkg}} = \ln 2 \; T \, \varepsilon \; \frac{x \, \eta \, N_A}{\mathscr{M}_A} \; \frac{M \, T}{n_L}. \tag{6}$$

Every future experiment on $0\nu\beta\beta$ has as one of its major goals the reach of the zero background condition (see the discussion in section 7) since, as it can be seen by comparing Equations (4) and (6), the sensitivity increases faster in the latter case, namely linearly with the exposure (the product of the detector mass times the live time).

Within the natural isotopic composition of the different elements, we find 69 $\beta\beta$-unstable nuclides present [3]. However, only a small subset is of any practical experimental interest for the study of $0\nu\beta\beta$. In fact, the choice for a suitable candidate is driven by multiple important requirements:

1. a high $Q_{\beta\beta}$, since this corresponds to a higher decay probability, due to the higher Phase Space Factor, and to a lower beta-gamma natural radioactive background,
2. a good detector energy and time resolutions, together with a long enough half-life of the $2\nu\beta\beta$ half-life, to avoid excessive background counts from this dominating channel;
3. a large natural isotopic abundance or an affordable possibility to isotopically enrich the material;
4. the compatibility with a well-established detection technique.

Unfortunately each of these requests implies often contradictory constraints and a compromise solution is usually unavoidable. As a result, the list of isotopes commonly under study includes [4]: ^{48}Ca, ^{76}Ge, ^{82}Se, ^{96}Zr, ^{100}Mo, ^{116}Cd, ^{130}Te, ^{136}Xe, and ^{150}Nd. Among these, ^{130}Te presents important advantages (**Table 1**) and it results to be a very favorable choice. The $Q_{\beta\beta}$ of ^{130}Te lies in between the Compton edge and the full-energy peak of the 2615 keV γ-line from ^{208}Tl and therefore in a quite low natural background region, while the long $2\nu\beta\beta$ half-life (about $8 \cdot 10^{20}$ yr [9]) limits the hiding effects of the unavoidable background from this process over the sought peak.

The isotopic abundance of ^{130}Te is more than 30% in natural Te, a value by far larger than that of all the other above-mentioned isotopes, and a further enrichment is viable, as it has been successfully demonstrated [11]. At the same time, ^{130}Te can be part of many different detectors: scintillators [12], solid state detectors [13, 14], as passive source in a tracker-calorimeter detector [15] or in a liquid scintillator [16]. But the most powerful application for the ^{130}Te $0\nu\beta\beta$ study remains at present the use of TeO_2 thermal detectors.

[1]This is true for instance if impurities are uniform inside the detector. But this might not be always the case. For example, if the main background component is superficial, it is the surface over volume ratio that matters. Also, the external background does not scale with the mass since the outer layers of the detector act as a shielding for the core part.

TABLE 1 | Relevant features of ^{130}Te for the search of $0\nu\beta\beta$.

^{130}Te properties	
$Q_{\beta\beta}$ [keV], [5–8]	2527.515 ± 0.013 †
$2\nu\beta\beta$ half-life [10^{20} yr], [9]	8.2 ± 0.2 (stat.) ± 0.6 (syst.)
nat. isot. abundance (%), [10]	34.167 ± 0.002
affordability	
^{nat}Te [$/kg], [a]	45
^{enr}Te (95% ^{130}Te) [$/kg], [b]	20,000

[a] *https://www.metalprices.com*
[b] *Private communication with Prof. F. Avignone*
† *Combined value from the weighted mean of the individual results.*

2. BOLOMETRIC TECHNIQUE

Bolometers are calorimeters in which the energy released in a crystal, acting as absorber, by an interacting particle is converted into phonons and measured via temperature variation. These detectors can operate only at cryogenic temperatures of about 10 or few tens of mK. The elementary excitation energy transferred to the lattice phonon system is of the order of 10 meV, which corresponds, in the typical detectors used for $0\nu\beta\beta$ searches, to a temperature increase of about a few tens/hundreds of μK per MeV.

The idea behind the phonon-mediated particle detection is very simple: the specific heat C of a dielectric and diamagnetic crystal cooled down to the millikelvin region can be so low that appreciable temperature increases are induced even by the tiny energy released during a single particle interaction. At these temperatures, C is proportional to the cube of the ratio between the operating and the Debye temperatures of the absorber crystal. In a very intuitive approach, a bolometer can be sketched as a device consisting of an energy absorber thermally linked to a thermometer (**Figure 1**). A weak thermal link, of conductance G, between the detector and a heat sink kept at constant temperature T_S is needed in order to restore the original temperature after the impinging of the particle. Of course, the real situation is much more complex. For example, the parameters C and G should not be considered as global quantities, but rather as the sum of many contributions, each with its specific behavior. Anyway, this simple thermal model will suffice in order to get a general idea about the operation of these devices.

If a certain amount of energy E is released in the absorber, it will produce a change in temperature ΔT equal to the ratio between E and C. Let $T(t)$ be the absorber temperature as a function of the time t and let us assume that

$$\Delta T \equiv |T(t) - T_S| \ll T_S \quad \forall t, \tag{7}$$

so that C and G can be considered constant quantities. The temperature variation can then be described by the time evolution

$$\Delta T(t) = \frac{E}{C}\, e^{-t/\tau} \quad \text{where} \quad \tau \equiv \frac{C}{G}. \tag{8}$$

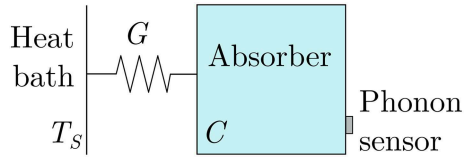

FIGURE 1 | Simplified bolometer thermal model. The detector is modeled as a single object with heat capacity C coupled to the heat sink (at constant temperature T_S) through the thermal conductance G. The phonon sensor plays no active role.

The characteristic time of the thermal pulse can be very long, up to few seconds, depending on the values of C and G. From Equation (8) we can see that, to get a large signal amplitude, C has to be as small as possible. C is therefore a crucial parameter in the design of the detector.

For what concerns the intrinsic energy resolution of a thermal detector, the only limiting factor are the fluctuations of the internal energy of the system due to the continuous phonon exchange between the absorber and the heat sink. At the thermal equilibrium, the mean number of phonons will be $N = C(T)/k_B$, each with mean energy $\varepsilon = k_B\, T$ [17], and therefore:

$$\Delta E \propto \varepsilon \sqrt{N} = \xi \sqrt{k_B\, C(T)\, T^2}. \tag{9}$$

The factor ξ is a dimensionless factor that depends on the details of the real detector and it can become of the order of unity with a proper optimization work. Equation (9) tells that the intrinsic energy resolution of bolometers can be as low as few eV even for crystal masses of the order of 1 kg, provided that the temperature is sufficiently low. This description shows that the resolution is independent of the energy released in the absorber. It holds only if we can assume that the system has reached a complete thermalization before the readout. In general, this is not always the case. For example, when the thermometer detects the out-of-equilibrium high-energy phonons directly produced by the particle interaction in the absorber, the energy resolution will be dominated by the fluctuation in the number of produced elementary quanta (phonons or quasi-particles, depending on the specific device). However, all the TeO_2 bolometers developed in the last 30 years for $0\nu\beta\beta$ search have been using semiconductor thermistors glued on the absorber crystals, for which the hypothesis of complete phonon thermalization before readout is quite correct.

In reality, the effective energy resolution of thermal detectors is generally dominated by the "extrinsic" noise generated by a variety of uncorrelated sources that cannot be fully eliminated [18, 19]. Among these we can cite the thermal noise (i.e., noise due to temperature instabilities of the heat sink), the Johnson noise, or any kind of noise related to the electronics readout and the cryogenic system. At the end, the combination of these multiple factors usually results in an energy resolution of the order of few keV at 1 MeV (see section 4), a value still competitive with that of the best performing detectors.

Besides the excellent performance, another important advantage of bolometers is the very broad choice for the absorber

material. Indeed, for almost any element it is possible to identify a compound suitable for a bolometric application. This is the case, for example, of Tellurium. In its metallic form, Te is unable to stand thermal cycles [20]. Instead, the compound Tellurium dioxide, TeO_2 has demonstrated to be an excellent choice, as it will be shown in sections 4 and 5.

The main disadvantages of bolometers are their intrinsic slow response and insensitivity to the nature of the interacting particles. However, the former can be mitigated by a proper choice of field of the application, such as rare-event searches, while the latter can take advantage by the acquisition of additional information. Hybrid detectors, characterized by the simultaneous measurement of heat and ionization or scintillation/Čerenkov light, had been proposed since long time [21]. These have already been successfully implemented in a number of experiments aiming at the detection of Dark Matter candidates [22–24]. At the same time, by exploiting the broad variety of available materials offered by the bolometric approach, a number of successful R&D's [11, 25–31] has demonstrated the effectiveness of this technique in the identification of the contributions from alpha emissions. This allows to get rid of one of the most dangerous background sources in experiments looking for $0\nu\beta\beta$, and it is thus paving the road to future low background experiments. Correspondingly, very sensitive light bolometric detectors have been developed [32–35] and implemented in medium-scale demonstrators [30, 36, 37] to demonstrate the viability of the technique. Molybdenum if at the moment the favorite choice even if tellurium is still a viable alternative.

3. TEO_2 BOLOMETERS FOR $0\nu\beta\beta$ STUDIES

As mentioned, the main component of a bolometer is the crystal acting as absorber and, in this regard, TeO_2 is a particularly suitable material. TeO_2 is the most stable oxide of Te [38] and presents good thermal properties for cryogenic particle detectors. TeO_2 crystals are dielectric and diamagnetic, with a relatively high value of the Debye temperature ($\Theta_D = (232 \pm 7)$ K [39]). This leads to very low heat capacity at cryogenic temperatures which, we recall, is fundamental if you want a high energy resolution bolometer. Since the thermal expansion of TeO_2 is very close to that of copper [40, 41], its use in the mechanical support structure does not introduce excessive strain on the crystals during cool down.

TeO_2 crystals have mechanical and optical characteristics that match very well the requirements for thermal detectors. At the same time, significant developments in preparing powder out of this compound and in growing the crystals allow nowadays the production of almost perfect (bubble-free, crack-free and twin-free) crystal boules from which crystals with masses of the order of 750 g [42, 43] or more [44, 45] can be routinely obtained. TeO_2 satisfies also the tight requirements imposed on radiopurity: thanks to dedicated production lines for the raw powder synthesis, the crystal growth and the surface processing, crystals with bulk contamination of the order of 10^{-6} Bq kg^{-1} for ^{238}U and ^{232}Th, and with surface contamination levels of a few 10^{-9} Bq cm^{-2} for both ^{238}U and ^{232}Th [46, 47], are now achievable [43, 46].

The other key component of a bolometer is the phonon sensor. The type of device used in all the ^{130}Te cryogenic detectors reviewed in this work has always been Ge thermistors. In general, semiconductor thermistors consist of small Ge crystals with a region doped near the metal-insulator transition (MIT). The resistance presents therefore a steep slope as a function of the temperature, with a logarithmic sensitivity, $A \equiv |d \log R(T) / d \log T|$, that can reach values close to 5–10. To reach a very uniform and large dopant distribution, together with an accurate net dopant concentration, the Neutron Transmutation Doping (NTD) [48] technique can be used. The semiconductor slab, from where the thermistors will be afterwards obtained, is bombarded with a high intensity neutron flux, which induces nuclear transformations of some of the natural Ge isotopes. This leads to the formation of a compensated doped semiconductor, with n- and p- dopants present at a similar concentration level near the MIT. For brevity, these doped semiconductors are usually referred to as simply "NTDs." The resistivity as a function of the temperature follows the exponential law

$$\rho = \rho_0 \exp\left(\frac{T_0}{T}\right)^{\gamma} \tag{10}$$

where ρ_0 and T_0 are parameters that depend on the doping level and compensation. For NTDs γ is typically 1/2 [49].

The resistance variations of the thermistor are transformed into a readable voltage signal using a constant bias current I_B generated by means of the bias circuit shown in **Figure 2**. The DC power supply is closed on a load resistor R_L in series with the thermistor $R_{\rm bol}$, with $R_L \gg R_{\rm bol}$. In this way I_B is practically independent of the value of $R_{\rm bol}$. Once a certain bias current is circulating, a voltage drop $V_{\rm bol}(T) = I_B R_{\rm bol}(T)$ crosses the thermistor. The consequent power dissipation $P = I_B V_{\rm bol}$ produces a rise of the bolometer temperature $T_{\rm bol}$ and acts back on the resistance $R_{\rm bol}(T)$, lowering it, and therefore reducing the voltage drop. This in turn reduces the dissipated power, until an equilibrium is reached:

$$T_{\rm bol} = T_S + \frac{P}{G}. \tag{11}$$

This phenomenon causes the V-I relation, called "load curve," to deviate from the simple Ohm law and leads to a behavior that is often referred to as "electrothermal feedback." The (I_B , $V_{\rm bol}$) pair, once the equilibrium is reached, corresponds to a precise working point for the thermistor and any instantaneous temperature variation will be translated into a voltage pulse. The relationship between the electrical pulse height $\Delta V_{\rm bol}$ and the energy deposition E in the crystal is obtained by solving the circuit of **Figure 2**:

$$\Delta V_{\rm bol} \sim \frac{E}{C \cdot T_{\rm bol}} \cdot \sqrt{P \cdot R_{\rm bol}} \tag{12}$$

where P is the power dissipated in the thermistor $R_{\rm bol}$ by Joule effect.

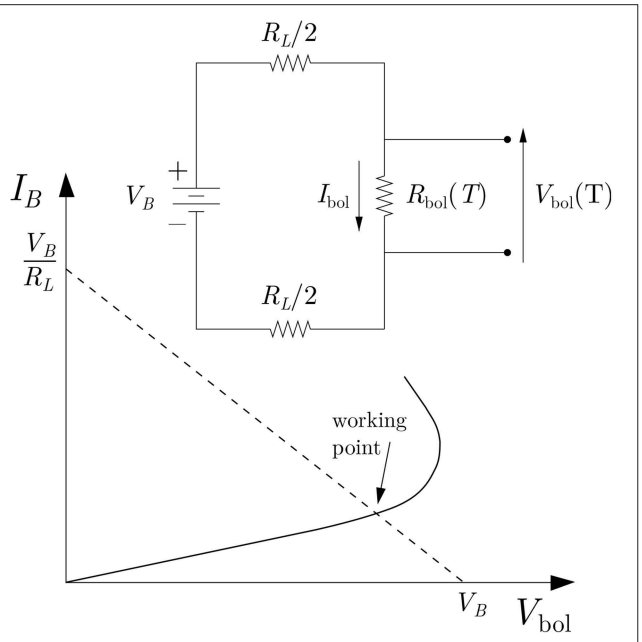

FIGURE 2 | (Top) Electric scheme of the biasing system used for the NTD readout. (Bottom) Typical load curve of a semiconductor thermistor. The working point is set as the intersection between the *V-I* characteristic curve and the load line $V_{\rm bol} = V_B - I_B R_L$.

The highest sensitivity in the conversion of the thermal pulse into an electric voltage signal is obtained when the working point is selected close to the inversion on the load curve (see **Figure 2**). Its value is way larger than the one that would be obtained by selecting a working point in the linear part of the load curve. To make a concrete example, an energy deposition of 1 MeV in a 750 g TeO_2 absorber at 10 mK typically produces a temperature increase $\Delta T \sim 100\,\mu$K, with a related voltage drop $\Delta V_{\rm bol} \sim 100\,\mu$V.

An additional crucial component of a thermal detector is the pulser system. When bolometers are operated over long periods, keeping a stable detector's response becomes mandatory, even in presence of temperature fluctuations of the cryogenic setup. In these cases, a pulser able to periodically deliver a fixed and extremely precise amount of energy to the detector [50, 51], represents an effective approach to deal with this issue. Of course, the system must generate a pulse as similar as possible to that corresponding to a real event. Such control pulses can be obtained by injecting calibrated amounts of energy through the interaction of well-known energetic charged particles, or by means of light pulses transmitted via optical fibers, or by Joule-heating of a resistive element thermally coupled to the absorber crystal. The variation of the detector response to the same energy deposition can then be used to correct (off-line) the effects of most of the cryogenic instabilities.

In the TeO_2 bolometers covered by this review, the chosen solution has been to glue on the crystal a resistive element consisting in a heavily doped (well above the MIT region) Si semiconductor, which thus exhibits a low-mobility metallic behavior [52]. This special "heater" satisfies two important requirements: to have a resistance free from temperature and applied voltage dependence, and a negligible heat capacity if compared to that of the crystal. This solution offers the clear advantage of a complete control on the off-line detector's response correction: the pulses can be released periodically and their rate and amplitudes can be chosen looking at the specific needs of the experiment. In order to provide an energy release as prompt as a real particle interaction would be, the relaxation time of the heat toward the crystal has to be much shorter than all the thermal time constants of the detector, while the signal generation of particle interactions and Joule-heating has to be similar enough to ensure that the pulse amplitude dependence on time, baseline level and other operation conditions, will be the same for the two processes.

Finally, the remaining components of any cryogenic detector are both the mechanical and electrical connections. Regarding the former, the mechanical holder of the TeO_2 crystals and the main thermal connection to the heat bath have been relying since long time on the use of more or less complex PTFE clamps and copper structures. By taking advantage of the different thermal contraction of these materials and of the crystals, it has been possible to fasten the system as a whole. Concerning the latter, electrical contacts are obtained by means of 25 or 50 μm-thick gold wires bonded on the thermistor and on the Si heater.

4. PAST EXPERIMENTS

A long sequence of measurements based on TeO_2 thermal detectors began to take place starting from 1991. The original group was led by E. Fiorini and comprised only a few researchers. Early runs were carried out with crystals with very small mass, from 6 g to 73 g [53–56]. Apart from the study of $0\nu\beta\beta$, these runs were intended to investigate the background level achievable with the bolometric technique, whose use was relatively new in the field. A large effort was thus paid to the mitigation of the background contamination of the whole experimental apparatus, by constantly improving the material selection and the design of the detector components.

These bolometric measurements found a favorable environment in the Laboratori Nazionali del Gran Sasso of I. N. F. N. (LNGS) in Italy[2]. With a rock coverage of about 3600 m w. e. and a mostly calcareous composition [57], this facility is able to guarantee very low muon and neutron fluxes, at the level of $3 \cdot 10^{-8}\,{\rm cm}^{-2}\,{\rm s}^{-1}$ [58] and $4 \cdot 10^{-6}\,{\rm cm}^{-2}\,{\rm s}^{-1}$ [59], respectively, thus offering suitable conditions for the search for $0\nu\beta\beta$.

The results obtained on the $0\nu\beta\beta$ half-life of ^{130}Te immediately showed to be competitive and world-leading. In less than 2 years since the start of the experimental activity, it was possible to improve the limit coming from a direct search from $t^{0\nu}_{1/2} > 2.8 \cdot 10^{18}$ yr (obtained with a CdTe detector [13]) to $t^{0\nu}_{1/2} > 2.7 \cdot 10^{21}$ yr at 90% C. L. [56], and to pass the most stringent at the time, i.e., $t^{0\nu}_{1/2} > 2.6 \cdot 10^{21}$ yr, coming from an

[2]https://www.lngs.infn.it/en

inclusive double beta decay study ($0\nu\beta\beta + 2\nu\beta\beta$) of ^{130}Te with the geochemical method [60].

A significant improvement was represented by the use of a $3 \times 3 \times 6\,cm^3$ TeO_2 crystal of 334 g of mass [61] (at the time, the largest thermal detector ever operated in the world), that became the unitary element of the first bolometric array with large-mass crystals. In particular, a detector constituted by 4 bolometers was operated in 1994 [62], while a tower made of 20 bolometers (5 floors of 4 crystals each) was assembled and operated since 1997 [63]. The latter experiment was named MiDBD (Milan Double Beta Decay) and opened the competitive era of bolometers in the world leadership ride for $0\nu\beta\beta$ searches.

MiDBD proved that an energy resolution of 5 keV at $Q_{\beta\beta}$ was within reach and achieved a very low background of less than 1 counts $keV^{-1}\,kg^{-1}\,yr^{-1}$ in the Region of Interest (ROI), around $Q_{\beta\beta}$. After few years of operation, the original detector was dismounted and remounted in a new and significantly improved configuration [64]. The new crystal assembly was much more compact and it was therefore possible to reinforce the detector shielding with additional lead. Moreover the new design required less support material for the crystals (copper and PTFE), thus allowing to reduce the background even more thanks to less passive material mass and surface and a more effective anti-coincidence analysis. With a total exposure of 4.25 kg yr, MiDBD set the limit $t^{0\nu}_{1/2} > 2.1 \cdot 10^{23}$ yr at 90% C. L. .

In parallel with the operation of MiDBD, an important technological improvement was obtained with the massive production of very high quality crystals of $\sim$ 750 g and their successful operation as bolometers [65]. These $5 \times 5 \times 5\,cm^3$ TeO_2 crystals were proposed as "bricks" of an extremely ambitious project: a bolometer array of 1000 cryogenic detectors, the Cryogenic Underground Observatory for Rare Events, alias CUORE [66]. The unitary element of such a big array was supposed to be a tower of 4-crystal floors, similar to MiDBD but with bigger crystals.

As an intermediate step toward CUORE, a single tower, named Cuoricino (Italian for "small CUORE") was designed and operated. Apart from being a proof of concept for CUORE, Cuoricino was with full honors a standalone experiment. The tower, the new world largest cryogenic detector ever in operation, consisted of 44 $5 \times 5 \times 5\,cm^3$ crystals, and 18 $3 \times 3 \times 6\,cm^3$ crystals coming from MiDBD, for a total TeO_2 mass of 40.7 kg. These crystals were disposed into 13 floors, 11 4-crystal modules housing the larger crystals and 2 9-crystal modules housing the smaller ones.

The detector was successfully run for over 5 years. The best performance, both in terms of background counts and resolution, was reached with the 5 cm-side bolometers, which achieved (0.153 ± 0.006) counts $keV^{-1}\,kg^{-1}\,yr^{-1}$ in the ROI[3] and a FWHM resolution of (5.8 ± 2.1) keV [70] at the $Q_{\beta\beta}$. Cuoricino improved the previous limit on $0\nu\beta\beta$ set by MiDBD by more than one order of magnitude: $t^{0\nu}_{1/2} > 2.8 \cdot 10^{24}$ yr at 90% C. L. . At the same time, this detector showed that it was possible to operate massive and complex bolometric detector arrays almost continuously.

In view of the forthcoming CUORE experiment, a big effort was paid to the investigation of the background sources. Thanks to Cuoricino, it was definitely confirmed that the major contribution to the counts in the ROI was produced by "degraded" alphas, i.e., alpha particles that deposit only part of their total energy in the detector, as expected in crystal or copper/PTFE surface events. Several dedicated R&D setups were put into operation in an ancillary cryostat at LNGS to investigate the individual contributions to the background, in order to address the issue of its reduction in the most effective way. These studies led to an improved detector design and cleaning protocol for both the crystals and the support materials. In addition, a completely industrialized assembly line was realized in order to transform the over 10,000 ultra-clean pieces into CUORE towers [71]: all the construction processes had to be performed into sealed glove boxes constantly flushed with N_2 to prevent the re-contamination of the various components by any exposure to air (and thus to Rn).

The final test for CUORE consisted in operating as a standalone experiment a prototype tower, CUORE-0, produced and assembled following all the new procedures, protocols and prescriptions. The CUORE-0 tower [70] comprised 52 $5 \times 5 \times 5\,cm^3$ crystals, arranged in 13 4-crystal floors, for a total mass of 39 kg of TeO_2. The collected data allowed ultimately to check all the improvements achieved since Cuoricino. In particular, for what concerns the background, a significant reduction was obtained, spanned over the whole energy range, with a factor $\sim$ 3 reduction in the $Q_{\beta\beta}$ region. The counts in the ROI were $(0.058 \pm 0.004\,(\text{stat.}) \pm 0.002\,(\text{syst.}))$ counts $keV^{-1}\,kg^{-1}\,yr^{-1}$ and the α continuum above 2615 keV was a factor $\sim$ 7 smaller than that obtained with Cuoricino.

The combined limit of Cuoricino and CUORE-0, whose results are comparable due to the better performance of the latter despite its shorter live time, was $t^{0\nu}_{1/2} > 4.0 \cdot 10^{24}$ at 90% C. L. [67], among the stringent ones on the $0\nu\beta\beta$ process.

5. PRESENT: THE CUORE EXPERIMENT

CUORE [72] consists of 19 CUORE-0-like towers. The number of TeO_2 crystals is 988, for a total mass of 742 kg (**Figure 3**). Given the natural isotopic abundance, this corresponds to $\sim$ 206 kg of ^{130}Te. CUORE is by far the largest bolometer array operated.

After the design and realization of the assembly line, the full detector construction took about 2 years. The installation inside the CUORE cryostat could be performed after the completion of the commissioning of the cryogenic system. In the meanwhile, the individual towers were stored in sealed containers constantly flushed with clean N_2 gas, inside the CUORE cleanroom. This prevented any contamination of the crystals and frames from Rn. The installation was performed during summer 2016. This extremely delicate task (the fragile detector is completely "bare") was carried out in a controlled cleanroom environment continuously flushed with Rn-free filtered air [73]. The background target

[3]The ROI can be intended as the 100 keV-wide region around $Q_{\beta\beta}$, namely (2470 − 2570) keV. In that energy region the 2505 keV ^{60}Co sum peak (see **Figure 6**) appears, but does not contribute to the background in the ROI.

FIGURE 3 | The CUORE detector with the experiment logo. Reproduced with permission from the CUORE Collaboration. See original in the official CUORE experiment website. Available online at: https://cuore.lngs.infn.it/en.

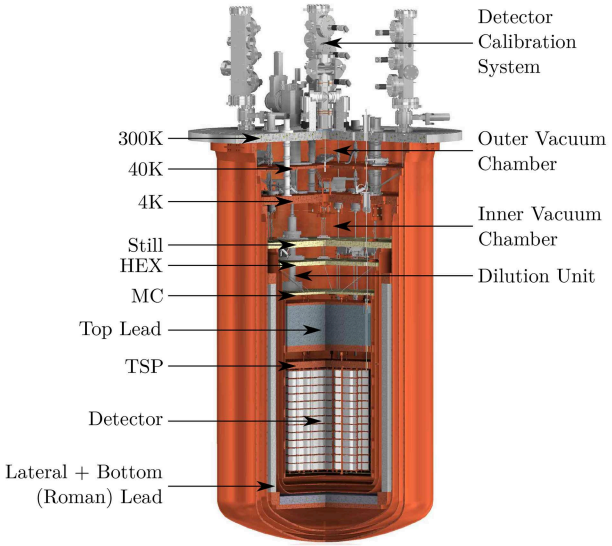

FIGURE 4 | The CUORE cryostat. The different thermal stages, the lead shields, the vacuum chambers and the cooling units are indicated. See original in the official CUORE experiment website. Available online at: https://cuore.lngs.infn.it/en.

level in the ROI was set to $0.01\,\text{counts}\,\text{keV}^{-1}\,\text{kg}^{-1}\,\text{yr}^{-1}$, reflecting the expected outcome of the extensive background reduction program.

CUORE also benefited from the completely new cryostat. The CUORE cryostat is a huge custom-made dilution refrigerator cooled down by multiple Pulse Tube units [74, 75]. Its design had to satisfy a set of very stringent experimental requirements: high cooling power and cryogenic reliability, low noise detector environment and extremely low radioactivity content. In particular, the cryostat is composed of six nested high-purity-copper vessels. The innermost vessel encloses the experimental volume, which is $\sim 1\,\text{m}^3$ (**Figure 4**). The detector is attached to a dedicated suspension system that strongly reduces the amount of transmitted vibrations, which represent a noise source. In order to mitigate the radioactive background, almost 7 t of lead are integrated in the structure. The largest part of the shielding is made of ancient Roman lead [76]. In addition, the whole apparatus is protected from the external environmental radioactivity by a 80-ton composed shield made of polyethylene, H_3BO_3 and lead.

CUORE, which started the data-taking in spring 2017, will collect data until reaching a total of 5 yr live time. The successful cool down and operation of CUORE marks an important step in the application of thermal detectors for rare-event searches, by bringing it to the ton-scale. It also opens the way to the use this technologies to future large-mass bolometer arrays.

5.1. CUORE Background

The experience acquired in running the previous TeO_2 experiments, supported by a complete Monte Carlo simulation of the detector (and of the shielding) that has been developed and fine-tuned step-by-step since MiDBD, allowed the implementation of a background model for CUORE-0 first [9], and then for CUORE [77]. Three dominant sources have been identified as contributors to the Background Index (BI):

- multi-Compton events from the γs line of ^{208}Tl (2615 keV), coming from the ^{232}Th contamination of the cryogenic system;
- ^{238}U and ^{232}Th α-emitting contamination (with related decay products), coming from the surface of the TeO_2 crystals. This also include the surface contamination ^{210}Pb (with the long half-life of $\sim$ 22.3 yr) from the environmental ^{222}Rn;
- α-emitting contamination coming from the surfaces of the inert materials facing the crystals, mostly the copper frames.

The strategy adopted in CUORE in order to reduce these contributions consisted in the optimization, i.e., reduction, of the amount of inert material employed for the detector frames and structure and in the improved design of the shields. This was done in addition to the dedicated cleaning treatments, both for crystals and copper. The resulting effectiveness has been demonstrated by CUORE-0, which observed a reduced background with respect to Cuoricino of about a factor 3 in the ROI. This success was actually limited by the use of the same cryogenic infrastructure of the Hall A cryostat (about 25-years-old during the run CUORE-0).

The selection and procurement of all the materials then used in the construction of the CUORE detector and cryostat was preceded by a broad screening campaign. This study employed different material assay techniques and considered both bulk and surface contamination (these could have occurred during the part handling and machining, and/or due to air exposure). Furthermore, a specific analysis of material activation for TeO_2 was performed. This helped to confirm that the overall exposure to cosmic radiation following the production and transportation of the crystals did not constitute a major issue for CUORE [78].

In the end, the sources that were believed could give a sizable contribution to the CUORE BI were identified with:

- ^{238}U and ^{232}Th (and their progeny) coming from crystals and holders;
- cosmogenically activated isotopes from crystals and copper parts closest to the detector;
- ^{238}U and ^{232}Th coming from cryostat vessels and lead shields.

The projection of the total BI resulted in $(1.02 \pm 0.03\,(\text{stat})^{+0.23}_{-0.10}\,(\text{syst})) \cdot 10^{-2}$ counts keV^{-1} kg^{-1} yr^{-1}. A detailed list of the individual contributions is reported in **Figure 5**. The dominant entry is represented by the degraded αs coming from the surface contaminants of the detector frames.

The ultimate validation (or rejection) of the projected background model for CUORE will come from the CUORE data themselves, provided that sufficiently high statistics will be collected.

5.2. CUORE First Results

At the end of 2017, CUORE released the first results on the $0\nu\beta\beta$ search. The total TeO_2 exposure was 86.3 kg yr [69]. The background was found in line with the expectations: $(1.4 \pm 0.2) \cdot 10^{-2}$ counts keV^{-1} kg^{-1} yr^{-1}, while the average bolometer energy resolution at $Q_{\beta\beta}$ was (7.7 ± 0.5) keV. The latter parameter saw an improvement during the data-acquisition campaign and room for further a improvement down to ~ 5 keV is still present, thanks to improved cryogenic stability and data analysis.

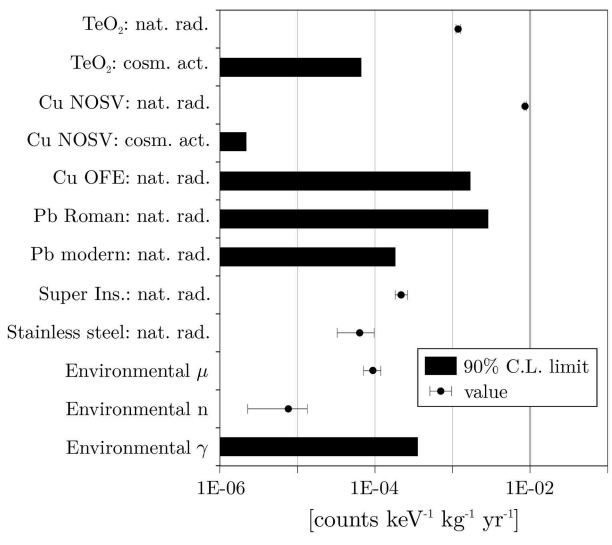

FIGURE 5 | Histogram with the main BI components expected for CUORE. The bars indicate upper limits (90% C. L.), while the markers derived values (with 1σ uncertainty). The thick line marks the CUORE background target. Figure from Alduino et al. [77].

The final spectra in ROI region for MiDBD, Cuoricino and CUORE-0 spectra are reported in **Figure 6**, together with the initial CUORE spectrum. The combined limit of CUORE, CUORE-0 and Cuoricino on the ^{130}Te $0\nu\beta\beta$ half-life is $1.5 \cdot 10^{25}$ yr [69]. It follows the corresponding limits in ^{136}Xe and ^{76}Ge, namely $1.1 \cdot 10^{26}$ yr at 90% C. L. by the KamLAND-Zen Collaboration [79] and $8.0 \cdot 10^{25}$ yr at 90% C. L. by the GERDA Collaboration [80]. Eventually, CUORE is expected to raise its half-life limit sensitivity at $9.0 \cdot 10^{25}$ yr at 90% C. L. [81], therefore ensuring the central role played by thermal detectors in the forthcoming future.

5.3. Constraints on the Neutrino Mass

The huge impact on Particle Physics that the observation of $0\nu\beta\beta$ would have is of course not related to the interest on an extremely rare nuclear decay, that would put another important tile in the framework of Nuclear Physics and would challenge theoreticians to explain the observed half-life, but to the consequences that the observation or even the limits posed on its half-life would have on neutrino physics.

The connection between $0\nu\beta\beta$ and some neutrino properties can be extracted from the Majorana effective mass definition:

$$m_{\beta\beta} \equiv \left| e^{i\alpha_1} |U_{e1}^2| m_1 + e^{i\alpha_2} |U_{e2}^2| m_2 + |U_{e3}^2| m_3 \right| \qquad (13)$$

where m_i are the masses of the neutrino eigenstates ν_i, $\alpha_{1,2}$ are the Majorana phases and U_{ei} are the elements of the PMNS mixing matrix that define the composition of the electron neutrino: $|\nu_e\rangle = \sum_{i=1}^{3} U_{ei}^* |\nu_i\rangle$.

If a $0\nu\beta\beta$ would be observed, the measurement of $t_{1/2}^{0\nu}$ would translate into a value of $m_{\beta\beta}$, while an experimental limit on $t_{1/2}^{0\nu}$ will always correspond to an upper bound on $m_{\beta\beta}$. In order to operate this conversion, it is necessary to pass through quantities obtained by theoretical calculations of atomic and nuclear physics. Within the hypothesis of "ordinary" neutrinos as mediators of the $0\nu\beta\beta$ transition, a convenient parametrization for $t_{1/2}^{0\nu}$ can be:

$$\left[t_{1/2}^{0\nu} \right]^{-1} = \frac{m_{\beta\beta}^2}{m_e^2} G_{0\nu} \, |\mathcal{M}_{0\nu}|^2 \qquad (14)$$

where $G_{0\nu}$ is the Phase Space Factor (PSF), $\mathcal{M}_{0\nu}$ is the Nuclear Matrix Element (NME), and m_e is the electron mass, conventionally taken as normalization factor for $m_{\beta\beta}$.

By inverting Equation (14) and by choosing proper values for the isotope of interest for PSF [82] and NME (e.g., [83]), it is thus possible to obtain the limits on $m_{\beta\beta}$ starting from the experimental sensitivities.

There has been a lot of discussions in the last years on the correct value of the axial-vector coupling constant to be used in the calculation of the NME and for this reason you will now

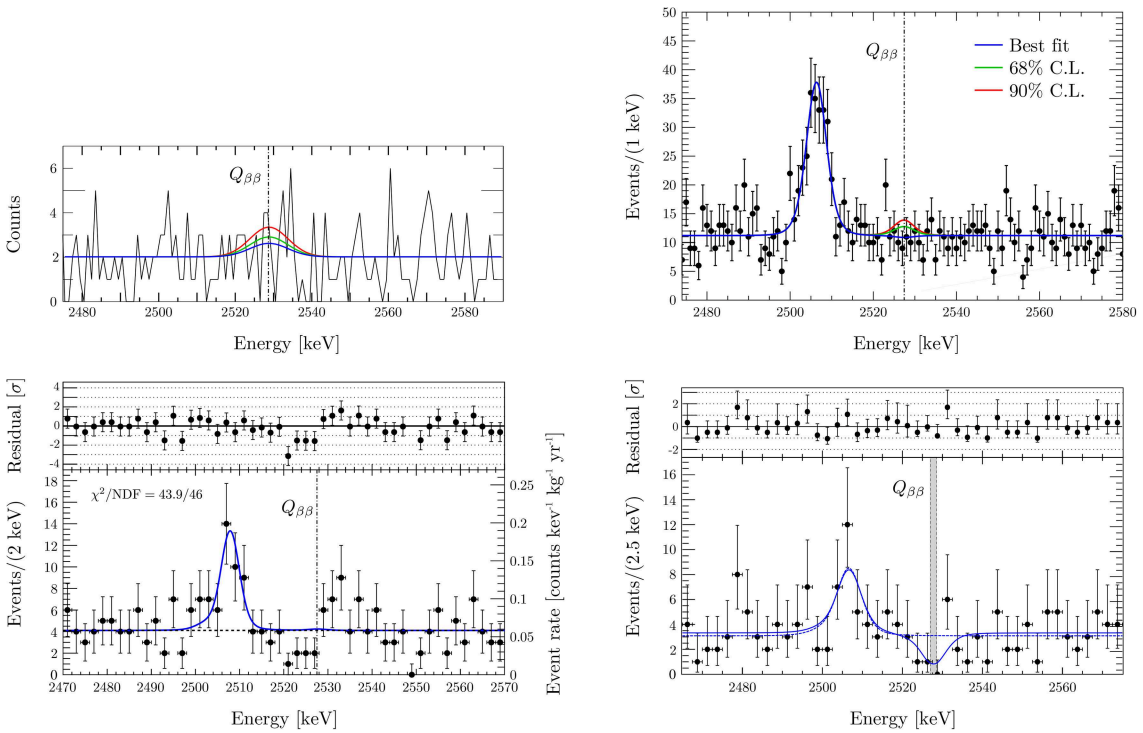

FIGURE 6 | (From Left to Right, Top to Bottom) MiDBD, Cuoricino, CUORE-0 and CUORE (first data release) best-fit model in the ROI region. No peak is found at $Q_{\beta\beta}$ (that at $\sim$ 2507 keV is attributed to ^{60}Co). Figures from Arnaboldi et al. [64], with permission from Elsevier, Alfonso et al. [67], with permission from Elsevier, Andreotti et al. [68], with permission from the American Physical Society, and Alduino et al. [69], with permission from the American Physical Society (see the references for details).

often find Equation (14) unfolded, with the dependence from g_A^4 made explicit. Since we still lack of a unanimous guideline on the value to be used for g_A in nuclear decays in general and in $0\nu\beta\beta$ in particular, we will stick to the conventionally used value of $g_{A,nucl} \simeq 1.27$, the value observed in neutron decay, leaving it hidden inside the NME.

When passing from $t_{1/2}^{0\nu}$ to $m_{\beta\beta}$, the uncertainties in the theoretical calculations should be taken into account. The PSFs have been recently recalculated [82] with accurate precision for most of the nuclei of interest for $0\nu\beta\beta$. The present uncertainty is about 7%. For the NMEs, the situation is more complicated. A relatively small intrinsic error of $\lesssim$ 20% [83, 84] is presently assessed by the most recent calculations within the same theoretical approach. But the disagreement between the results from different models is still quite large, up to a factor $\sim$ 3.

For this reason, any experimental limit on $t_{1/2}^{0\nu}$ will actually correspond to a range of values for $m_{\beta\beta}$, that will translate into a horizontal band in the usual representation of $m_{\beta\beta}$ as a function of the mass of the lightest neutrino $m_{lightest}$ [85, 86]. An example is shown in **Figure 7**. The two branches that appear in these type of plots correspond to the two (mutually exclusive) scenarios of Normal and Inverted Hierarchy (NH and IH) of the neutrino mass spectrum. The broadness of the branches depends on the adopted approach in discussing the theoretical uncertainties.

As for the experiments with TeO_2 discussed in this paper, their limits on $m_{\beta\beta}$, calculated using the PSF from Kotila and Iachello [82] and the NME from Barea et al. [83], are shown in **Table 2**. As can be seen, the evolution of the limit on the decay half-life of the $0\nu\beta\beta$ of ^{130}Te proceeded in parallel with the technological improvements on the bolometric detectors: mass, energy resolution, background.

In **Figure 7** the bands coming from some of the most studied isotopes are plotted. The constraint from ^{130}Te, i.e., the current CUORE limit on $m_{\beta\beta} < (110 - 520)$ meV [69], is already compatible with that from ^{76}Ge, while the projected CUORE sensitivity should reach (or pass) the most stringent present limit, coming from ^{136}Xe, approaching the Inverted Hierarchy region.

6. OTHER STUDIES

Although $0\nu\beta\beta$ of ^{130}Te is the main objective of TeO_2 bolometers, a number of other processes is open to experimental investigation. The excellent energy resolution and the anticipated low background rates allow competitive sensitivities for many of them. The accessible processes include alternative modes of double beta decay as well as more exotic processes predicted by some extensions of the SM.

Indeed, natural tellurium includes $\beta\beta$-active isotopes other than ^{130}Te, namely ^{120}Te and ^{128}Te, and the $\beta\beta$ transitions to excited states can provide unique information on the

$0\nu\beta\beta$ mechanism. On the other hand, the precise measurement of the $2\nu\beta\beta$ half-lives is crucial to test the constraints of the $\beta\beta$ nuclear matrix elements.

Among the exotic processes, the experimental investigation of the validity limits of fundamental principles such as the charge conservation or the CPT/Lorentz invariance deserve particular attention since most of our theoretical construction is based on them. On an equal footing, the search for Dark Matter candidates (which, by the way, began with the first $0\nu\beta\beta$ experiments), is still a subject on which TeO_2 bolometers can provide competitive results.

6.1. Alternative Double Beta Decays

Thanks to a larger available energy, the best $0\nu\beta\beta$ experimental sensitivity is generally for the transition to the ground state of the daughter nucleus. However double beta decay may occur (in both 2ν and 0ν modes) also to an excited state of the daughter nucleus. In the case of $0\nu\beta\beta$, these transitions can disclose the exotic mechanisms (e.g., RH currents) which mediate the decay [89, 90], while for $2\nu\beta\beta$ they can provide unique insight to the details of the mechanisms responsible for the nuclear transition [91, 92]. From the experimental point of view, most of the interest is motivated by the fact that in a close packed array, like those developed for TeO_2 bolometers, the strong signature provided by the simultaneous detection of one or two gammas can lead to an almost background-free search. In this respect, the transitions to 0^+ states are favored while states with larger spin (e.g., 2^+) are generally suppressed by angular momentum conservation. The adopted strategy exploits multiple coincidence patterns to select topological configurations characterized by a lower background contribution [93]. In this respect, particularly interesting is the $0\nu\beta\beta$ transition of ^{130}Te to the 0^+ excited state at 1793.5 keV of ^{130}Xe whose de-excitation is characterized by a cascade of multiple high energy gamma's which provide distinctive signatures.

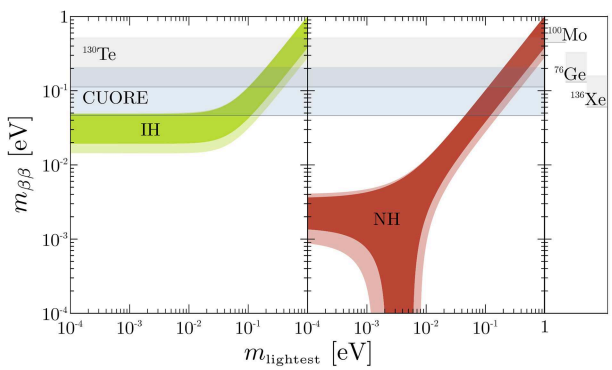

FIGURE 7 | Predictions on $m_{\beta\beta}$ from oscillations as a function of the mass of the lightest neutrino in the two cases of NH and IH. The shaded areas correspond to the 3σ regions after propagation of the uncertainties on the oscillation parameters [87]. The horizontal gray band shows the current $0\nu\beta\beta$ limit of ^{130}Te after the first CUORE data release [69], while the blue band shows the projected CUORE sensitivity [81]. To the side, the current limits on the $0\nu\beta\beta$ half-life for ^{76}Ge [80], ^{100}Mo [88] and ^{136}Xe [79] are reported.

Up to date, no evidence for any of the $\beta\beta$ transitions of tellurium isotopes to 0^+ and 2^+ excited states of xenon has been observed. In all the cases, the most stringent limits come from TeO_2 bolometers [63, 93–96]. The 90% C. L. half-life limits by the combined Cuoricino + CUORE-0 are [93]:

$$\tau^{0\nu}_{0^+} > 1.4 \cdot 10^{24}\,\text{yr} \quad \text{and} \quad \tau^{2\nu}_{0^+} > 2.5 \cdot 10^{23}\,\text{yr}. \tag{15}$$

^{130}Te is certainly the most favorable isotope for $\beta\beta$ searches (see section 5.3).

Two other tellurium isotopes are however also $\beta\beta$ -active: ^{128}Te and ^{120}Te . ^{120}Te can β^+EC decay to ^{120}Sn with a transition energy of 1730 keV [97]. Despite $\beta^+\beta^+$, β^+EC and EC EC modes are generally less appealing because of the lower available energy, they can only be mediated by peculiar mechanisms and can therefore provide unique details on the decay [98, 99]. Although no calculation of the nuclear matrix element is presently available in the literature for ^{120}Te , the expected $0\nu\beta^+$EC half-lives for other most commonly investigated isotopes are a few orders of magnitude larger with respect to $0\nu\beta\beta$, making the search for this decay mode very appealing. In addition, the presence of the positron with the consequent emission of a pair of back-to-back 511 keV gammas provides extremely clean signatures (**Figure 8**) which reduce the background contributions and compensate for the low isotopic abundance of ^{120}Te (0.09%). The decay scheme is:

$$^{120}\text{Te} + e^- \rightarrow {}^{120}\text{Sn}^* + \beta^+ \rightarrow {}^{120}\text{Sn} + X + \beta^+ \rightarrow {}^{120}\text{Sn} + X + 2\gamma, \tag{16}$$

TABLE 2 | Main characteristics of the TeO_2 bolometric experiments searching for the $0\nu\beta\beta$ of ^{130}Te.

Experiment	Crystals	Mass [kg]	Exposure† [kg yr]	BI in ROI [counts keV^{-1} kg^{-1} yr^{-1}]	FWHM at $Q_{\beta\beta}$ [keV]	$t^{0\nu}_{1/2}$ (90% C. L.) [y]	$m_{\beta\beta}$ [eV]
MiDBD [64]	20	6.8	4.25	0.6 (Run I) / 0.3 (Run II)	5 – 15	$2.1 \cdot 10^{23}$	1.6
Cuoricino [68, 70]	62	40.7	71.4	0.20 (Run I) / 0.15 (Run II)	5.8 ± 2.1	$2.8 \cdot 10^{24}$	0.43
CUORE-0 [67]	52	39.0	35.2	0.058 ± 0.004	4.9 ± 2.9	$4.0 \cdot 10^{24}$	0.36
CUORE (first data) [69]	988	742	86.3	0.014 ± 0.002	7.7 ± 0.5	$1.5 \cdot 10^{25}$	0.19
CUORE (expected) [81]	988	742	3705	0.01	5	$9.0 \cdot 10^{25}$	0.076

† *Total exposure of TeO_2. To get the corresponding exposure of ^{130}Te, it is sufficient to multiply the value per $\simeq 0.278$, with the exceptions of MiDBD and Cuoricino, which contained enriched crystals.*

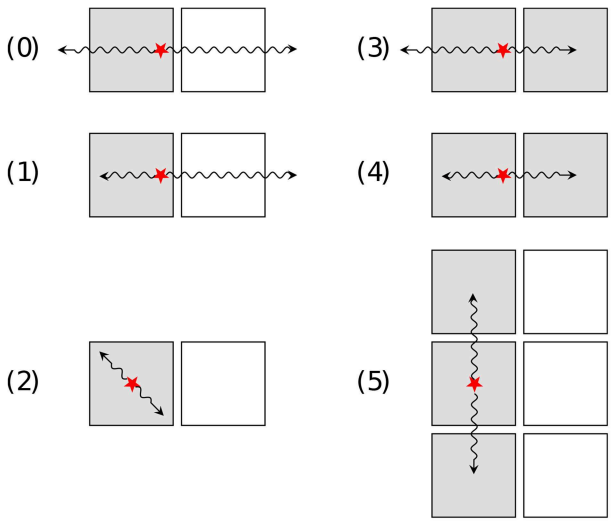

FIGURE 8 | Signatures of the $0\nu\beta^+$EC decay of ^{120}Te in CUORE-0. The red stars indicated the energy depositions by the β^+ , while the arrows represent the resulting annihilation 511-keV γ rays. The shaded squares show the crystals which see an energy deposition. Figure from Alduino et al. [100], with permission from the American Physical Society.

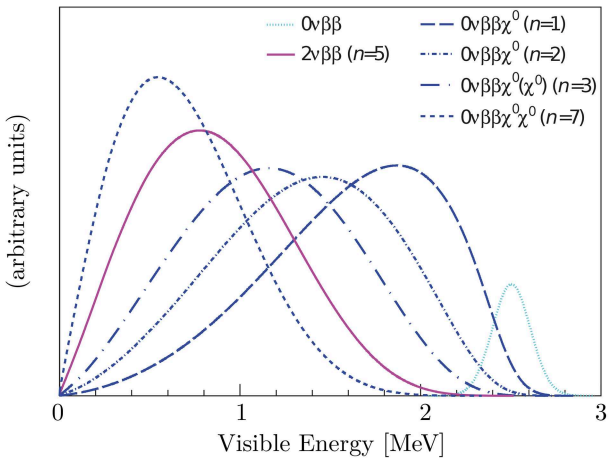

FIGURE 9 | Visible $0\nu\beta\beta$ with Majoron emission energy spectra for different spectral index n in the case of ^{136}Xe. The line at $Q_{\beta\beta}$, charaterized by the KamLAND-Zen detector resolution, indicates the position of the $0\nu\beta\beta$ peak without Majoron emission. Figure from Gando et al. [106], with permission from the American Physical Society.

where the asterisk indicates an atomic excited state while X stays for the products of atomic de-excitation (X-rays or Auger electrons). In TeO_2 bolometers the latter amounts to the captured electron binding energy and adds to the positron energy. The signature is therefore the coincidence of a fixed amount of energy deposition and two 511 keV γs. No evidence for ^{120}Te decay has been observed so far, and again the stringent limits is set by TeO_2 bolometers, namely the combined Cuoricino + CUORE-0 [100, 101]:

$$t^{0\nu}_{1/2}(^{120}\text{Te}) > 2.7 \cdot 10^{21}\ \text{yr (90\% C. L.)}. \tag{17}$$

^{128}Te $\beta\beta$ transitions have been investigated since a long time. The large natural isotopic abundance of this isotope, 31.74%, is in fact very appealing. However the very low transition energy, 866.6 keV [97], leads to a generally poor sensitivity and weakens the interest for this search. On the other hand, its very large $2\nu\beta\beta$ half-life [102] is out of reach even for a ton-sized arrays like CUORE.

Exotic $0\nu\beta\beta$ forms, characterized by the emission of a massless Goldstone boson, called Majoron, were originally introduced within SM extensions in which neutrino masses are obtained as a manifestation of the spontaneous break of the lepton number symmetry [103]. The precise measurements of the Z invisible width at LEP, has greatly disfavored the original Majoron triplet and pure doublet. Several new models have been developed [104, 105], which predict different (continuous) spectral shapes for the sum energies of the emitted electrons. This extends from zero to the transition energy $Q_{\beta\beta}$: $dN/dT \propto (Q_{\beta\beta} - T)^n$, where T is the electron summed kinetic energy and the spectral index n depends on the decay details (**Figure 9**). Single Majoron emissions are characterized by $n = 1-3$, while double Majoron decays can have either $n = 3$ or $n = 7$. The precise measurement of n allows to discriminate between the processes and $2\nu\beta\beta$ ($n = 5$). As for any process characterized by continuous spectra, the experimental sensitivity is mainly limited by the background contributions and the detector mass. Several experiments looking for $0\nu\beta\beta$ have focused their attention on these exotic searches [106–109]. In the case of TeO_2 bolometers, stringent half-life limits on these exotic decays have been set by past arrays [63], namely

$$\tau^{0\nu}_{\text{Majoron}} > 1.4 \cdot 10^{21}\ \text{yr}\ (n = 1) \quad \text{and} \quad > 7.0 \cdot 10^{20}\ \text{yr}\ (n = 2) \tag{18}$$

while competitive results are anticipated by future extensions of the technology based on the simultaneous detection of Čerenkov light and aiming at unprecedented reductions of the background [110, 111].

$2\nu\beta\beta$ is a direct transition between isobaric nuclei differing by two units of nuclear charge and corresponds to two simultaneous beta decays:

$$(A, Z) \rightarrow (A, Z + 2) + 2e^- + 2\bar{\nu}_e. \tag{19}$$

It is an allowed process within the SM and was originally proposed based on the observed trend of nuclear masses in isobaric multiplets [112]. $2\nu\beta\beta$ is the slowest nuclear decay ever discovered. It has actually been observed in a number of candidate nuclei. Most of the interest for this decay mode arises from its similarity with $0\nu\beta\beta$ (compare Equation 19 to Equation 11). Indeed, the calculation of the nuclear matrix elements for the latter are the main source of uncertainty in the extraction of the relevant neutrino parameters and it is expected that $2\nu\beta\beta$ experimental results could provide relevant insight into the details of these calculations (see section 5.3). However, in practice the $2\nu\beta\beta$ experimental results have further complicated the situation: the measured $2\nu\beta\beta$ half-lives have outlined an evident

disagreement with calculations. An explanation is still missing as well as how this disagreement affects $0\nu\beta\beta$ calculations.

From the experimental point of view, the $2\nu\beta\beta$ represents an irreducible source of background for the $0\nu\beta\beta$ searches. The finite energy resolution of the detector produces a smearing of the spectrum which brings some $2\nu\beta\beta$ events in the $0\nu\beta\beta$ region. Thanks to the excellent energy resolution of bolometers and to the relatively long $2\nu\beta\beta$ half-life of ^{130}Te , this will not be a concern even for next generation TeO_2 experiments. However, a potential issue for thermal detectors is constituted by the random coincidences of $2\nu\beta\beta$ events [113, 114]. The resulting pile-up would not be disentangled due to the bad time resolution which, in the case of TeO_2 bolometers with NTD thermistors, is of the order of 1 ms at best. Nonetheless, this contribution is estimated to be $< 10^{-4}$ counts keV^{-1} t^{-1} yr^{-1} for a 1 t TeO_2 experiment with enriched crystals [115], or even less in case a light signal would also be recorded (see section 7), and it is thus negligible.

TeO_2 thermal detectors have provided the most precise measurements of ^{130}Te $2\nu\beta\beta$ half-life [9, 64, 116]. **Figure 10** shows the fit obtained with the background simulation in CUORE-0 (left panel) and CUORE first data release (right panel). The contribution of the $2\nu\beta\beta$ is clearly visible in both spectra. In particular, in CUORE, this accounts for nearly all of the signal in the range (1–2) MeV. The extracted value for the ^{130}Te $2\nu\beta\beta$ is [116]:

$$t_{1/2}^{2\nu} = (7.9 \pm 0.1\,(\text{stat.}) \pm 0.2\,(\text{syst.})) \cdot 10^{20}\,\text{yr}. \tag{20}$$

6.2. Violation of Fundamental Principles

The decay of an atomic electron is probably the most sensitive test of electric charge conservation. Charge Non Conservation (CNC) can be obtained by including additional interactions of leptons and photons which can lead to the decay of the electron:

$$e \rightarrow \gamma\, \nu_e \quad \text{or} \quad e \rightarrow \nu_e\, \nu_X\, \bar{\nu}_X. \tag{21}$$

These modes conserve all known quantities but electric charge. An additional possibility is connected with CNC involving interactions with nucleons. Discussions of CNC in the context of gauge theories can be found in a number of Beyond SM gauge theories [117–119].

Referring to Equation (21), while the signature of the three-neutrino mode is quite poor, the coincidence between the decay γ and the atomic de-excitation X-rays can give rise to interesting topological configurations. These can help to lower the background contributions and look particularly suited for bolometric arrays with a high granularity. The most stringent limits on CNC have been obtained as side results in experiments characterized by large masses and very low backgrounds [120, 121]. Indeed, the large detection efficiency, low threshold and excellent energy resolution of TeO_2 bolometers are crucial to detect the low energy de-excitation X-rays or Auger electrons. The sensitivity has been so far limited by the available mass so that competitive results are anticipated by CUORE and future developments of this technique.

Lorentz invariance and CPT violations arising from the spontaneous breaking of the underlying space-time symmetry are interesting theoretical feature that can be parametrized within SM extensions [122–124]. Lorentz-violating effects in the neutrino sector can thus appear both in the 2ν and 0ν decay modes [125]. A distortion of the two-electron summed energy is expected for $2\nu\beta\beta$ due to an extra term in the phase space factor, while $0\nu\beta\beta$ could be directly induced by a Lorentz-violating term. The experimental signature is therefore very similar to the one expected for Majoron searches with a deformation of the $2\nu\beta\beta$ spectrum [125]. This investigation has been recently performed by the EXO Collaboration on ^{136}Xe [126]. A similar study is foreseen for CUORE, and dedicated analysis tools have already been developed [127].

The Pauli Exclusion Principle (PEP) is one of the basic principles of Physics, upon which modern atomic and nuclear physics are built. Despite its well known success, the exact validity of PEP is still an open question, and an experimental verification is thus extremely important [128]. Indeed, a number of experimental investigations have been carried out both in the nuclear and atomic sector [129–132]. Each time, the signature is a transition to an already occupied (atomic or nuclear) level which is clearly prohibited by the PEP. Dedicated searches to the PEP exploit the continuous filling of atomic levels with fresh electrons in order to measure the corresponding X-ray transitions to occupied levels. Instead, most of the low activity experiments uses large masses and/or low background rates to search for the emission of specific "wrong energy" electromagnetic or nuclear radiation from atoms or nuclei. TeO_2 bolometers, belonging to the latter category, take advantage of the excellent energy resolution to isolate the seeked X-ray lines. However, sensitivity has been so far mainly limited by the detector mass and competitive results are therefore expected only for future generation ton-sized arrays. Unfortunately, a model linking the various experimental observations is still missing and a comparison of the sensitivities is therefore difficult, and must carefully take into account the assumptions underlying the specific search [133].

Baryon number (B) conservation is an empirical symmetry of the SM and its violation is predicted by a number of extensions. In particular, some of these theoretical frameworks, which allow for small neutrino masses, anticipate $\Delta B = 3$ transitions in which three baryons can simultaneously disappear from the nucleus, often leaving an unstable isotope [134]. The coincidence between the tri-nucleon decay and the radioactive decay of the daughter nuclei is thus a robust signature for TeO_2 arrays and can help to get rid of the backgrounds. The dominant $\Delta B = 3$ decay modes are:

$$\text{ppp} \rightarrow e^+\pi^+\pi^+,\ \text{ppn} \rightarrow e^+\pi^+,\ \text{pnn} \rightarrow e^+\pi^0,\ \text{nnn} \rightarrow \bar{\nu}\pi^0. \tag{22}$$

These can be experimentally investigated by exploiting the decay specific energy and time constraints. Recently, results on the search for instability of bound nucleons have been reported for ^{136}Xe [135] and for ^{76}Ge [136]. The half-life limits range, depending on the decay mode, around 10^{23} yr in the former case, and around 10^{25} yr in the latter one.

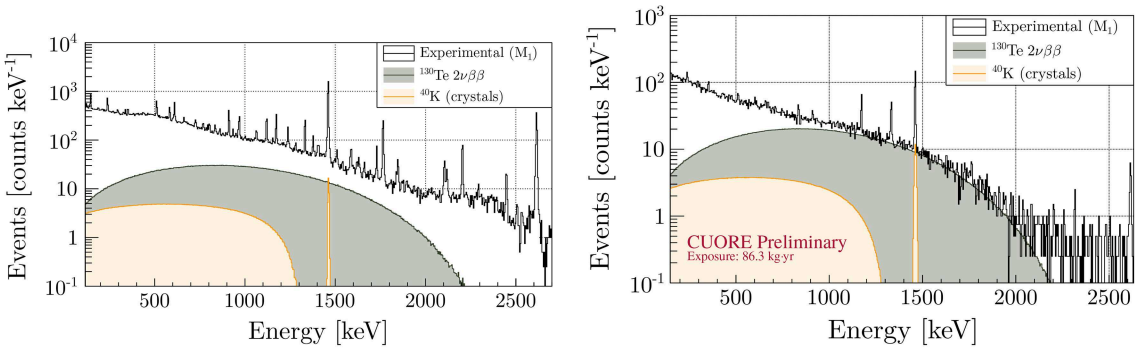

FIGURE 10 | CUORE-0 (Left) and CUORE first data release (Right) spectra compared to the $2\nu\beta\beta$ contribution predicted by the reference fits. The ^{40}K peak from the crystal contamination (the radioactive source that has the strongest correlation with the $2\nu\beta\beta$) is also reported. Figures from Alduino et al. [9] and Ouellet [116].

6.3. The Rare Nuclear Decay of ^{123}Te

Primordial radionuclides are nuclides characterized by lifetimes longer than the time passed since their formation. Therefore, they are still surviving today. Besides the progenitors of the natural decay series, ^{232}Th, ^{235}U and ^{238}U, this set comprises: ^{40}K, ^{87}Rb, ^{115}In, ^{123}Te, ^{138}La, ^{144}Nd, ^{147}Sm, ^{148}Sm, ^{174}Hf, ^{176}Lu, ^{187}Re, and ^{190}Pt. Their rare nuclear decays are generally of interest not only for nuclear spectroscopy but also for the implications of the very long lifetime in geochronology and ore dating. Furthermore, despite expected to occur based on the available mass measurements, the β decays of few isobaric doublets are still missing experimental observation and are often characterized by conflicting results.

This is the case for ^{123}Te , which is expected to decay by EC to the ground state of ^{123}Sb with a second forbidden unique transition ($Q = 51.3$ keV). Indeed, published lower limits on the lifetime of this decay [137, 138] are in contradiction with the positive result of $1.23 \cdot 10^{13}$ yr, quoted in most of the papers on the subject [139]. The reason for the disagreement is still unclear, but it is probably due to limits imposed by the original experimental technique. If the limits were confirmed, or even more stringent ones would be set, then ^{123}Te could be characterized by the longest natural single β transition, a fact of obvious interest for nuclear physics.

The main advantage of TeO_2 thermal detectors is to implement a pure calorimetric approach, characterized by a distinctive signature in which the signal corresponds to an energy release equal to the binding energy of the captured electron. The most probable capture is then from the L3 atomic shell, with an energy of 4.1 keV. The EC decay of ^{123}Te has been investigated in a number of TeO_2 bolometric measurements. Initial limits on the suppressed K-capture [138] has been later improved when technological improvements have contributed to lower the detector threshold, thus allowing the study of the L-capture processes [140]. Here a signal corresponding to another highly suppressed L1 capture has been observed leaving the question of the ^{123}Te decay existence still open. It is expected that CUORE (and possible future TeO_2 developments), thanks to the increased mass and lower background will finally contribute to provide a definite answer.

7. LOOKING AHEAD

CUORE is not the ultimate bolometric experiment searching for $0\nu\beta\beta$. On the contrary, it represents a crucial step toward the forthcoming generation of experiments. Thanks to the knowledge acquired by running the first ton-scale bolometric detector, we are now aware of where and how to intervene in order to further increase the sensitivity. It appear realistic to imagine a next-generation $0\nu\beta\beta$ experiment hosted inside the CUORE cryogenic infrastructure.

As discussed in section 2, thermal detectors offer a wide choice for the possible absorber materials, hence isotopes different from ^{130}Te can be as well considered due to their "intrinsic" properties and/or to the more favorable characteristics of the outcoming detector. Indeed, such scenario is an open possibility concerning a post-CUORE experiment (see [115]). Anyhow, TeO_2 still remains a valid choice, and the following discussion will focus on the search for $0\nu\beta\beta$ of ^{130}Te with this latter compound.

As shown in section 1, the detector sensitivity for the search of $0\nu\beta\beta$ is determined by the live time of the experiment, the mass of isotope under observation, the detector energy resolution and the background level. These are therefore the key quantities to address to improve the sensitivity. In particular, all next-generation forthcoming experiments aim at reaching the zero background condition, and this sets very stringent requirements on the detector features and performance, i.e., the relation in Equation (5) must hold.

In order to increase the total mass of ^{130}Te, we could in principle allocate more crystals by further optimizing the detector design. However, we must keep in mind that this option is eventually constrained by the experimental volume available in the CUORE cryostat. Alternatively (or combined), we could use TeO_2 crystals enriched in ^{130}Te: this would correspond to an increase in the isotope mass of almost a factor 3. The results in this direction are promising. Apart from the pioneering studies on enriched crystals with MiDBD and CUORICINO, the recent bolometric run of two TeO_2 crystals enriched at $\sim$ 92% in ^{130}Te showed that performance comparable to CUORE-0 are within reach [11]. Specifically, these crystals (of mass $\sim$ 435 g each) exhibited a FWHM energy resolution of 6.5 and 4.3 keV (at the

^{208}Tl line). Moreover, no contamination in ^{232}Th was observed, while a small contamination of ^{238}U was present, still more than 10 times larger than that of the CUORE crystals. Therefore, some extreme purification procedure should be foreseen to avoid spoiling the excellent results achieved by the CUORE crystal quality. Some work in this direction has already started.

Concerning the live time of a future $0\nu\beta\beta$ experiment, given that it is quite unlikely that the data taking will last longer than a few years, it is important to maximize the experimental duty cycle in order to, in turn, maximize the exposure. A value larger than 80% has already been achieved by CUORE-0. Furthermore, the use of mechanical cryo-cooler in the CUORE cryostat (see section 5) additionally increases the total duty cycle compared to a LHe bath cryostat, such as the one used until CUORE-0, avoiding the need of refill. It sounds reasonable to expect to keep a duty cycle of about 80% also for a future experiment.

As discussed in section 2, bolometers fully exploit the potentiality of solid state detectors. Energy resolutions of the order of the per mille at the $Q_{\beta\beta}$, quite close to those of HPGe detectors, can be achieved.

Trying to improve the single detector performance—remind that the effective resolution of a bolometer is due to various noise sources, while in principle intrinsic value for CUORE-like bolometers should be of the order of some tens of eV—requires a deeper understanding of the thermal behavior. Studies aiming at reproducing the actual response of the CUORE bolometers have been carried out [141–143], while a large amount of data is becoming available thanks to CUORE. This will provide important information in this direction. However, we do not really know the level of improvement we can expect and, especially, when this will provide a practical contribution to the experimental search. The value of 5 keV, achieved by CUORE-0, still is a valid target for a forthcoming experiment.

The mitigation of the background is leading way toward the zero background condition. It actually represents the largest challenge we will deal with and it in fact is the target of most of the R&D projects which studying the optimal configuration/technology for a new generation bolometric detector. As it will be shown, there is still room for a significant improvement from the 0.01 counts keV^{-1} kg^{-1} yr^{-1} of CUORE.

7.1. Active Rejection of Background

In CUORE, the study of coincidences among events generated in nearby crystals allows to discard a significant fraction of α interactions and multi-Compton scatters of γs by rejecting simultaneous signals (within 10 ms) [69]. The main limitation of this method is that, in this way, it is only possible to identify events that deposit energy in multiple crystals. Therefore, despite the rejection efficiency is still high thanks to the detector compactness, the goal for a next-generation detector is to perform an active reduction of background against α events.

A very promising approach in this sense foresees a simultaneous readout of heat and light signals. In fact, by measuring the ratio of the emitted light over the dissipated energy (heat), it is possible to discriminate between β/γ and α events with the same energy, since the scintillation light is strongly quenched in the latter case. The combined readout can be obtained by coupling the main bolometer to a thin, large-area Ge or Si light detector (acting as well as a bolometer). The light collection can be maximized by wrapping the main crystal with a reflecting foil (**Figure 11**).

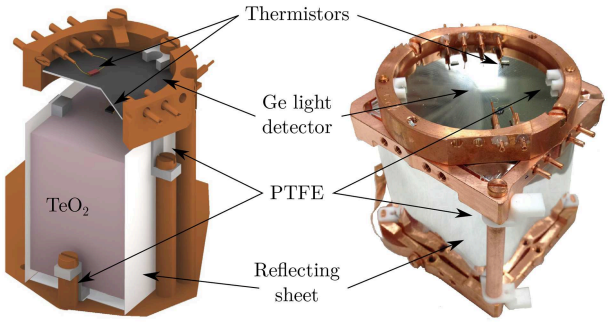

FIGURE 11 | Example of TeO_2 bolometers coupled to light detectors, allowing for a simultaneous measurement of heat + light signals. The crystals are wrapped with a reflecting foil to maximize light collection. Figures from Artusa et al. [11] and Casali et al. [144].

Despite this approach is limited to scintillating compounds, and noticeable results have already been obtained (see e.g., [30, 145, 146]), it can also be applied to TeO_2 crystals. In this case, the low luminescence of paratellurite is, at least partially, compensated by the suitable optical properties of the crystal to act as excellent Čerenkov radiators [147]. The Čerenkov emission threshold is $\sim$ 400 MeV for α particles while only $\sim$ 50 keV for electrons: no light emission is thus expected from the α background, allowing for a complete rejection. At the same time, $\sim$ 125 photons in the range (350 − 600) nm are expected for electron pair emitted in the $0\nu\beta\beta$ process, showing the challenge of this approach, even if it is feasible.

7.2. CUPID

The CUPID project, acronym for CUORE Upgrade with Particle IDentification [110] aims at constructing a bolometric $0\nu\beta\beta$ experiment with sensitivity on $t^{0\nu}_{1/2}$ of the order of $(10^{27} - 10^{28})$ yr at 90% C. L., starting from the experience and the expertise acquired by running CUORE. The largest efforts of CUPID is put into the identification of an effective strategy for a dramatic reduction of the background in the $0\nu\beta\beta$ ROI. In the case of TeO_2, the background suppression is pursued by developing high-quality light detectors, with sufficiently elevated performance to effectively identify Čerenkov emission.

Among the different technologies under investigation, we find the use of transition edge sensors [148, 149], microwave kinetic inductance detectors [150, 151], or Neganov-Trofimov-Luke (NTL) amplified light detectors [11, 33, 111, 149, 152, 153]. The results coming out from the several R&D programs are encouraging. As a remarkable example, in Bergé et al. [111] the authors demonstrate a complete event-by-event α *vs.* β/γ discrimination in a TeO_2 CUORE-like bolometer by employing a NTL-assisted Ge bolometer for the light collection (**Figure 12**).

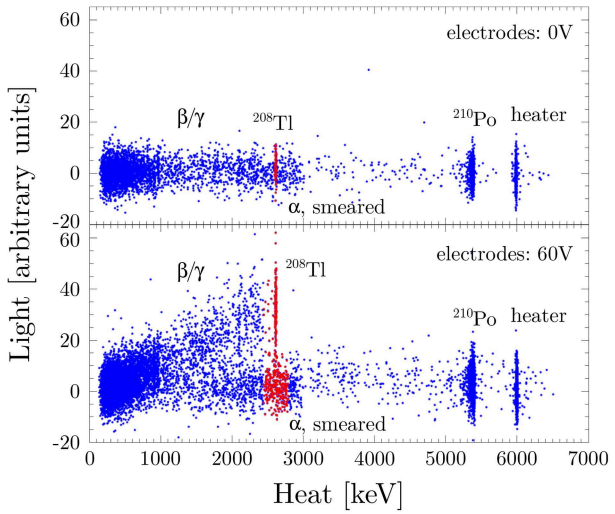

FIGURE 12 | Heat vs. light scatter plots obtained with a CUORE bolometer in coincidence with a NTL Ge light detector. (Top) The light detector is operated as a "standard" bolometric light detector, i.e., without applying any electrode voltage bias. (Bottom) The light detector working in a signal amplification regime, by applying 60 V as electrode bias. This results in a clear separation between α and β/γ signals. Figure from Bergé et al. [111], with permission from the American Physical Society.

At the same time, additional studies within the CUPID frame aim at tagging of surface events. Surface events can represent a problem if they become a significant background component, since in thermal detector there is no dead layer and the crystal surface is as sensitive as the bulk. In order to mitigate this background, an effective solution could be represented by the addition of a passive element on the bolometer surface. The coating may be obtained by deposition of a superconducting Al film, which would affect the shape of the signal events generated a few mm from the surface, thus making it possible be able to discriminate between bulk and surface events [154]. Alternatively, by wrapping the crystal with a scintillating foil, surface events could be identified by the measurement of scintillation light (which would be collected in addition to the Čerenkov light) generated by the interaction with the foil [155]. These solutions, together with strategies for the mitigation of the environmental radioactivity [156], could in principle translate into a dramatic reduction of the BI, of about two orders of magnitude with respect to CUORE. The level of 0.1 counts $keV^{-1}\ t^{-1}\ yr^{-1}$ is compatible with the zero background condition (see section 5.2) for a ton-size bolometric experiment.

8. SUMMARY

TeO_2 thermal detectors satisfy the experimental requirements needed by a competitive search for $0\nu\beta\beta$. This very important process—its discovery would directly address the open issues of the lepton number conservation and the Majorana nature of the neutrino—is in fact under study in a bunch of candidate isotopes, including ^{130}Te.

A long series of successful measurements at LNGS allowed to continuously improve the sensitivity on the half-life of the ^{130}Te $0\nu\beta\beta$. Today, the CUORE experiment is providing one of the most stringent limits in the field, namely $1.5 \cdot 10^{25}$ yr at 90% C. L.. At the same time, TeO_2 thermal detectors were used in different studies of rare nuclear processes, spanning from different $0\nu\beta\beta$ modes to the investigation of fundamental Physics laws.

Numerous R&Ds are paving the way for a next generation bolometric experiment searching for $0\nu\beta\beta$ with zero background and enhanced sensitivity, in the range of $(10^{27} - 10^{28})$ yr, showing that TeO_2 thermal detectors could continue to play a central role.

AUTHOR CONTRIBUTIONS

Each of the three authors has given an equivalent contribution to the writing of the different sections of the paper. However, each section has been reviewed, complemented, and corrected by the other authors. CB and OC have mainly conveyed their 30 year long experience in the field, while SD, stimulated by his direct contribution to the CUORE-0 and CUORE effort, has contributed a lot of enthusiasm in re-discovering and creating a new interest for the series of results which have lead to the modern approach to low temperature detectors for double beta decay.

ACKNOWLEDGMENTS

This review reports the successful results achieved by the CUORE (and previously Cuoricino) Collaborations. We therefore thank the numerous researchers and members of the technical staff of the institutions involved in this scientific enterprise.

REFERENCES

1. Furry WH. On transition probabilities in double beta-disintegration. *Phys Rev.* (1939) **56**:1184–93. doi: 10.1103/PhysRev.56.1184
2. Fukugita M, Yanagida T. Baryogenesis without grand unification. *Phys Lett B.* (1986) **174**:45. doi: 10.1016/0370-2693(86)91126-3
3. Tretyak VI, Zdesenko YG. Tables of double beta decay data: an update. *At Data Nucl Data Tables.* (2002) **80**:83–116. doi: 10.1006/adnd.2001.0873
4. Giuliani A, Poves A. Neutrinoless double-beta decay. *Adv High Energy Phys.* (2012) **2012**:857016. doi: 10.1155/2012/857016
5. Rahaman S, Elomaa VV, Eronen T, Hakala J, Jokinen A, Kankainen A, et al. Double-beta decay Q values of Cd-116 and Te-130. *Phys Lett B.* (2011) **703**:412–6. doi: 10.1016/j.physletb.2011.07.078
6. Redshaw M, Mount BJ, Myers E, Avignone FT. Masses of Te-130 and Xe-130 and Double-beta-Decay Q Value of Te-130. *Phys Rev Lett.* (2009) **102**:212502. doi: 10.1103/PhysRevLett.102.212502
7. Scielzo ND, Caldwell S, Savard G, Clark JA, Deibel CM, Fallis J, et al. Double-β decay Q values of ^{130}Te, ^{128}Te, and ^{120}Te. *Phys Rev C.* (2009) **80**:025501. doi: 10.1103/PhysRevC.80.025501
8. Nesterenko DA, Blaum K, Block M, Droese C, Eliseev S, Herfurth F, et al. Double$-\beta$ transformations in isobaric triplets with mass numbers A = 124,

130, and 136. *Phys Rev C.* (2012) **86**:044313. doi: 10.1103/PhysRevC.86.044313

9. Alduino C, Alfonso K, Artusa DR, Avignone FT, Azzolini O, Banks TI, et al. Measurement of the two-neutrino double beta decay half-life of ^{130}Te with the CUORE-0 experiment. *Eur Phys J C.* (2017) **77**:13. doi: 10.1140/epjc/s10052-016-4498-6
10. Meija J, Coplen TB, Berglund M, Brand WA, De Bièvre P, Gröning M, et al. Isotopic compositions of the elements 2013 (IUPAC Technical Report). *Pure Appl Chem.* (2016) **88**:293–306. doi: 10.1515/pac-2015-0503
11. Artusa DR, Avignone FT, Beeman JW, Dafinei I, Dumoulin L, Ge Z, et al. Enriched TeO_2 bolometers with active particle discrimination: towards the CUPID experiment. *Phys Lett B.* (2017) **767**:321–9. doi: 10.1016/j.physletb.2017.02.011
12. Zdesenko YG. On lepton charge conservation in the double β decay of ^{130}Te. *JETP Lett.* (1980) **32**:58.
13. Mitchell LW, Fisher PH. Rare decays of cadmium and tellurium. *Phys Rev C.* (1988) **38**:895–9. doi: 10.1103/PhysRevC.38.895
14. Ebert J, Fritts M, Gehre D, Goßling C, Hagner C, Heidrich N, et al. Results of a search for neutrinoless double-β decay using the COBRA demonstrator. *Phys Rev C.* (2016) **94**:024603. doi: 10.1103/PhysRevC.94.024603
15. Arnold R, Augier C, Baker J, Barabash AS, Basharina-Freshville A, Blondel S, et al. Measurement of the double beta decay half-life of ^{130}Te with the NEMO-3 detector. *Phys Rev Lett.* (2011) **107**:062504. doi: 10.1103/PhysRevLett.107.062504
16. Biller SD. Probing Majorana neutrinos in the regime of the normal mass hierarchy. *Phys Rev D* (2013) **87**:071301. doi: 10.1103/PhysRevD.87.071301
17. Moseley SH, Mather JC, McCammon D. Thermal detectors as x-ray spectrometers. *J Appl Phys.* (1984) **56**:1257. doi: 10.1063/1.334129
18. Mather J. Bolometer noise: nonequilibrium theory. *J Appl Opt.* (1982) **21**:1125. doi: 10.1364/AO.21.001125
19. Mather J. Bolometers: ultimate sensitivity, optimization, and amplifier coupling. *J Appl Opt.* (1984) **23**:584. doi: 10.1364/AO.23.000584
20. Alessandrello A, Brofferio C, Camin DV, Cremonesi O, Fiorini E, Giuliani A, et al. A Cryogenic tellurium detector for rare events and gamma-rays. *Phys Lett B.* (1990) **247**:442–7. doi: 10.1016/0370-2693(90)90923-T
21. Alessandrello A, Bashkirov V, Brofferio C, Bucci C, Camin DV, Cremonesi O, et al. A scintillating bolometer for experiments on double beta decay. *Phys Lett B.* (1998) **420**:109–13. doi: 10.1016/S0370-2693(97)01544-X
22. Abdelhameed AH, Angloher G, Bauer P, Bento A, Bertoldo E, Bucci C, et al. First results from the CRESST-III low-mass dark matter program (2019). arXiv [Preprint]. *arXiv:1904.00498*. Available online at: https://arxiv.org/abs/1904.00498 (submitted March 31, 2019).
23. Arnaud Q, Armengaud E, Augier C, Benot A, Bergé L, Billard J, et al. Optimizing EDELWEISS detectors for low-mass WIMP searches. *Phys Rev D.* (2018) **97**:022003. doi: 10.1103/PhysRevD.97.022003
24. Agnese R, Anderson AJ, Aramaki T, Asai M, Baker W, Balakishiyeva D, et al. New results from the search for low-mass weakly interacting massive particles with the CDMS low ionization threshold experiment. *Phys Rev Lett.* (2016) **116**:071301. doi: 10.1103/PhysRevLett.116.071301
25. Arnaboldi C, Beeman JW, Cremonesi O, Gironi L, Pavan M, Pessina G, et al. $CdWO_4$ scintillating bolometer for Double Beta Decay: light and Heat anticorrelation, light yield and quenching factors. *Astropart Phys.* (2010) **34**:143–50. doi: 10.1016/j.astropartphys.2010.06.009
26. Arnaboldi C, Capelli S, Cremonesi O, Gironi L, Pavan M, Pessina G, et al. Characterization of ZnSe scintillating bolometers for double beta decay. *Astropart Phys.* (2011) **34**:344–53. doi: 10.1016/j.astropartphys.2010.09.004
27. Gironi L, Arnaboldi C, Beeman JW, Cremonesi O, Danevich FA, Degoda VY, et al. Performance of $ZnMoO_4$ crystal as cryogenic scintillating bolometer to search for double beta decay of molybdenum. *J Intrum.* (2010) **5**:P11007. doi: 10.1088/1748-0221/5/11/P11007
28. Beeman JW, Bellini F, Cardani L, Casali N, Dafinei I, Di Domizio S, et al. Performances of a large mass ZnSe bolometer to search for rare events. *J Intrum.* (2013) **8**:P05021. doi: 10.1088/1748-0221/8/05/P05021
29. Cardani L, Cardani L, Casali N, Nagorny S, Pattavina L, Piperno G, et al. Development of a Li_2MoO_4 scintillating bolometer for low background physics. *J Intrum.* (2013) **8**:P10002. doi: 10.1088/1748-0221/8/10/P10002
30. Armengaud E, Augier C, Barabash AS, Beeman JW, Bekker TB, Bellini F, et al. Development of ^{100}Mo-containing scintillating bolometers for a high-sensitivity neutrinoless double-beta decay search. *Eur Phys J C.* (2017) **77**:785. doi: 10.1140/epjc/s10052-017-5343-2
31. Nagorny S, Pattavina L, Kosmyna MB, Nazarenko BP, Nisi S, Pagnanini L, et al. $^{arch}PbMoO_4$ scintillating bolometer as detector to searches for the neutrinoless double beta decay of ^{100}Mo. *J Phys Conf Ser.* (2017) **841**:012025. doi: 10.1088/1742-6596/841/1/012025
32. Colantoni I, Cardani L, Casali N, Cruciani A, Bellini F, Castellano MG, et al. Design and fabrication of the second-generation KID-based light detectors of CALDER. *J Low Temp Phys.* (2018) **193**:726–31. doi: 10.1007/s10909-018-1905-4
33. Gironi L, Biassoni M, Brofferio C, Capelli S, Carniti P, Cassina L, et al. Cerenkov light identification with Si low-temperature detectors with sensitivity enhanced by the Neganov-Luke effect. *Phys Rev C.* (2016) **94**:054608. doi: 10.1103/PhysRevC.94.054608
34. Beeman JW, Bellini F, Casali N, Cardani L, Dafinei I, Di Domizio S, et al. Characterization of bolometric Light Detectors for rare event searches. *J Instrum.* (2013) **8**:P07021. doi: 10.1088/1748-0221/8/07/P07021
35. Novati V, Artusa DR, Avignone FT, Beeman JW, Dafinei I, Dumoulin L, et al. An innovative bolometric Cherenkov-light detector for a ouble beta decay search. *Nucl Instrum Meth A.* (2018) **912**:82–4. doi: 10.1016/j.nima.2017.10.058
36. Azzolini O, Barrera MT, Beeman JW, Bellini F, Beretta M, Biassoni M, et al. First result on the neutrinoless double-β decay of ^{82}Se with CUPID-0. *Phys Rev Lett.* (2018) **120**:232502. doi: 10.1103/PhysRevLett.120.232502
37. Alenkov V, Bae HW, Beyer J, Boiko RS, Boonin K, Buzanov O, et al. First results from the AMoRE-Pilot neutrinoless double beta decay experiment (2019).
38. Dutton WA, Charles Cooper W. The Oxides and Oxyacids of Tellurium. *Chem Rev.* (1966) **66**:657–75. doi: 10.1021/cr60244a003
39. Barucci M, Brofferio C, Giuliani A, Gottardi E, Peroni I, Ventura G. Measurement of low temperature specific heat of crystalline TeO_2 for the optimization of bolometric detectors. *J Low Temp Phys.* (2001) **123**:303–14. doi: 10.1023/A:1017555615150
40. White GK, Collocott S, Collins JG. Thermal properties of paratellurite (TeO_2) at low temperatures. *J Phys Condensed Matter.* (1990) **2**:7715–8. doi: 10.1088/0953-8984/2/37/015
41. Kroeger FR, Swenson CA. Absolute linear thermal-expansion measurements on copper and aluminum from 5 to 320 K. *J Appl Phys.* (1977) **48**:853–64. doi: 10.1063/1.323746
42. Chu Y, Li Y, Ge Z, Wu G, Wang H. Growth of the high quality and large size paratellurite single crystals. *J Cryst Growth* (2006) **295**:158–61. doi: 10.1016/j.jcrysgro.2006.08.009
43. Arnaboldi C, Brofferio C, Bryant A, Bucci C, Canonica L, Capelli S, et al. Production of high purity TeO_2 single crystals for the study of neutrinoless double beta decay. *J Cryst Growth.* (2010) **312**:2999–3008. doi: 10.1016/j.jcrysgro.2010.06.034
44. Arnaboldi C, Brofferio C, Bucci C, Gorla P, Pessina G, Pirro S. 1.3 kg bolometers to search for rare events. *Nucl Instrum Meth A.* (2005) **554**:300–5. doi: 10.1016/j.nima.2005.07.060
45. Cardani L, Gironi L, Beeman JW, Dafinei I, Ge Z, Pessina G, et al. Performance of a large TeO_2 crystal as a cryogenic bolometer in searching for neutrinoless double beta decay. *J Instrum.* (2012) **7**:P01020. doi: 10.1088/1748-0221/7/01/P01020
46. Alessandria F, Andreotti E, Ardito R, Arnaboldi C, Avignone FT, Balata M, et al. CUORE crystal validation runs: results on radioactive contamination and extrapolation to CUORE background. *Astropart Phys.* (2012) **35**:839–49. doi: 10.1016/j.astropartphys.2012.02.008
47. Alessandria F, Ardito R, Artusa DR, Avignone FT, Azzolini O, Balata M, et al. Validation of techniques to mitigate copper surface contamination in CUORE. *Astropart Phys.* (2013) **45**:13–22. doi: 10.1016/j.astropartphys.2013.02.005
48. Haller EE, Palaio NP, Rodder M, Hansen WL, Kreysa E. NTD germanium: a novel material for low temperature bolometers. In: Larrabee RD, editor. *Neutron Transmutation Doping of Semiconductor Materials*. Boston, MA: Springer US (1984). p. 21–36. doi: 10.1007/978-1-4613-2695-3_2
49. Shklovskii BI, Efros AL. *Electronic Properties of Doped Semiconductors.* Berlin; Heidelberg: Springer (1984). doi: 10.1007/978-3-662-02403-4

50. Alessandrello A, Brofferio C, Bucci C, Cremonesi O, Giuliani A, Margesin B, et al. Methods for response stabilization in bolometers for rare decays. *Nucl Instrum Meth A* (1998) **412**:454–64. doi: 10.1016/S0168-9002(98)00458-6
51. Arnaboldi C, Giachero A, Gotti C, Pessina G. A very high performance stabilization system for large mass bolometer experiments. *Nucl Instrum Meth A.* (2011) **652**:306–9. doi: 10.1016/j.nima.2010.09.151
52. Andreotti E, Brofferio C, Foggetta L, Giuliani A, Margesin B, Nones C, et al. Production, characterization, and selection of the heating elements for the response stabilization of the CUORE bolometers. *Nucl Instrum Meth A.* (2012) **664**:161–70. doi: 10.1016/j.nima.2011.10.065
53. Alessandrello A, Alessandrello A, Brofferio C, Camin DV, Cremonesi O, Fiorini E, et al. Large mass, low temperature, low background detectors. *Nucl Instrum Meth A.* (1992) **315**:263–6. doi: 10.1016/0168-9002(92)90713-E
54. Giuliani A, Alessandrello A, Brofferio C, Camin DV, Cremonesi O, Fiorini E, et al. A low temperature TeO_2 detector to search for double beta decay of ^{130}Te. In: Hegarty S, Potter K, Quercigh E, editors. *Proceedings of the Joint International Lepton Photon Symposium at High Energies (15th) and European Phys. Soc. Conf. on High-energy Phys.* Singapore: World Scientific, (1992). p. 670–672.
55. Alessandrello A, Brofferio C, Camin DV, Cremonesi O, Fiorini E, Gervasio G, et al. A search for neutrinoless double beta decay of ^{130}Te with a bolometric detector. *Nucl Phys B.* (1992) **28A**:229–32. doi: 10.1016/0920-5632(92)90177-T
56. Alessandrello A, Brofferio C, Camin DV, Cremonesi O, Fiorini E, Gervasio G, et al. Milano experiment on $0-\nu\ \beta\beta$ decay of ^{130}Te with a thermal detector. *Nucl Phys B.* (1993) **31**:83–7. doi: 10.1016/0920-5632(93)90118-P
57. Catalano PG, Cavinato G, Salvini F, Tozzi M. Structural analysis of the Gran Sasso Laboratories of INFN (in Italian). *Mem Soc Geol It.* (1986) **35**:647–55.
58. Ambrosio M, Antolini R, Auriemma G, Baker R, Baldini A, Barbarino GC, et al. Vertical muon intensity measured with MACRO at the Gran Sasso Laboratory. *Phys Rev D.* (1995) **52**:3793–802. doi: 10.1103/PhysRevD.52.3793
59. Best A, Görres J, Junker M, Kratz KL, Laubenstein M, Long A, et al. Low energy neutron background in deep underground laboratories. *Nucl Instrum Meth. A.* (2016) **812**:1–6. doi: 10.1016/j.nima.2015.12.034
60. Kirsten T, Richter H, Jessberger E. Rejection of Evidence for Nonzero Neutrino Rest Mass from Double Beta Decay. *Phys Rev Lett.* (1983) **50**:474–7. doi: 10.1103/PhysRevLett.50.474
61. Alessandrello A, Brofferio C, Camin DV, Cremonesi O, Fiorini E, Garcia E, et al. A New search for neutrinoless $\beta\beta$ decay with a thermal detector. *Phys Lett B.* (1994) **335**:519–25. doi: 10.1016/0370-2693(94)90388-3
62. Alessandrello A, Brofferio C, Cremonesi O, Garcia E, Giuliani A, Nucciotti A, et al. First tests on a large mass, low temperature array detector. *Nucl Instrum Meth A.* (1995) **360**:363–6. doi: 10.1016/0168-9002(94)01723-9
63. Alessandrello A, Brofferio C, Cremonesi O, Fiorini E, Giuliani A, Nucciotti A, et al. New experimental results on double beta decay of ^{130}Te. *Phys Lett B.* (2000) **486**:13–21. doi: 10.1016/S0370-2693(00)00747-4
64. Arnaboldi C, Brofferio C, Bucci C, Capelli S, Cremonesi O, Fiorini E, et al. A Calorimetric search on double beta decay of ^{130}Te. *Phys Lett B.* (2003) **557**:167–75. doi: 10.1016/S0370-2693(03)00212-0
65. Alessandrello A, Brofferio C, Cremonesi O, Fiorini E, Giuliani A, Nucciotti A, et al. A massive thermal detector for alpha and gamma spectroscopy. *Nucl Instrum Meth A.* (2000) **440**:397–402. doi: 10.1016/S0168-9002(99)00928-6
66. Fiorini E. CUORE: a cryogenic underground observatory for rare events. *Phys Rep.* (1998) **307**:309–17. doi: 10.1016/S0370-1573(98)00060-X
67. Alfonso K, Artusa DR, Avignone FT, Azzolini O, Balata M, Banks TI, et al. Search for neutrinoless double-beta decay of ^{130}Te with CUORE-0. *Phys Rev Lett.* (2015) **115**:102502. doi: 10.1103/PhysRevLett.115.102502
68. Andreotti E, Arnaboldi C, Avignone FT, Balata M, Bandac I, Barucci M, et al. ^{130}Te neutrinoless double-beta decay with CUORICINO. *Astropart Phys.* (2011) **34**:822–31. doi: 10.1016/j.astropartphys.2011.02.002
69. Alduino C, Alfonso K, Andreotti E, Arnaboldi C, Avignone FT, Azzolini O, et al. First results from CUORE: a search for lepton number violation via $0\nu\beta\beta$ Decay of ^{130}Te. *Phys Rev Lett.* (2018) **120**:132501. doi: 10.1103/PhysRevLett.120.132501
70. Alduino C, Alfonso K, Artusa DR, Avignone FT, Azzolini O, Balata M, et al. CUORE-0 detector: design, construction and operation. *J Instrum.* (2016) **11**:P07009. doi: 10.1088/1748-0221/11/07/P07009
71. Buccheri E, Capodiferro M, Morganti S, Orio F, Pelosi A, Pettinacci V. An assembly line for the construction of ultra-radio-pure detectors. *Nucl Instrum Meth A.* (2014) **768**:130–40. doi: 10.1016/j.nima.2014.09.046
72. Artusa DR, Avignone FT, Azzolini O, Balata M, Banks TI, Bari G, et al. Searching for neutrinoless double-beta decay of ^{130}Te with CUORE. *Adv High Energy Phys.* (2015) **2015**:879871. doi: 10.1155/2015/879871
73. Benato G, G Biare D, Bucci C, Di Paolo L, Drobizhev A, Kadel RW, et al. Radon mitigation during the installation of the CUORE $0\nu\beta\beta$ decay detector. *J Instrum.* (2018) **13**:P01010. doi: 10.1088/1748-0221/13/01/P01010
74. Dell'Oro S. *Optimization of the CUORE detector during the commissioning phase*. (Ph. D. thesis). INFN - Gran Sasso Science Institute, l'Aquila, Italy (2017).
75. Alduino C, Alessandria M F Balata, Biare D, Biassoni M, Bucci C, et al. The CUORE cryostat: a 10 mK infrastructure for large bolometric arrays. (2019). *arXiv [Preprint]. arXiv:1904.05745*.
76. Alessandrello A, Arpesella C, Brofferio C, Bucci C, Cattadori C, Cremonesi O, et al. Measurements of internal radioactive contamination in samples of roman lead to be used in experiments on rare events. *Nucl. Instrum. Meth. B.* (1998) 142:163–72. doi: 10.1016/S0168-583X(98)00279-1
77. Alduino C, Alfonso K, Artusa DR, Avignone FT, Azzolini O, Banks TI, et al. The projected background for the CUORE experiment. *Eur Phys J C* (2017) **77**:543. doi: 10.1140/epjc/s10052-017-5080-6
78. Barghouty AF, Brofferio C, Capelli S, Clemenza M, Cremonesi O, Cebrián S, et al. Measurements of proton-induced radionuclide production cross sections to evaluate cosmic-ray activation of tellurium. *Nucl Instrum Meth B.* (2013) **295**:16–21. doi: 10.1016/j.nimb.2012.10.008
79. Gando A, Gando Y, Hachiya T, Hayashi A, Hayashida S, Ikeda H, et al. Search for majorana neutrinos near the inverted mass hierarchy region with KamLAND-Zen. *Phys Rev Lett.* (2016) **117**:082503. doi: 10.1103/PhysRevLett.117.109903
80. Agostini M, Bakalyarov AM, Balata M, Barabanov I, Baudis L, Bauer C, et al. Improved limit on neutrinoless double-β decay of ^{76}Ge from GERDA phase II. *Phys Rev Lett.* (2018) **120**:132503. doi: 10.1103/PhysRevLett.120.132503
81. Alduino C, Alfonso K, Artusa DR, Avignone FT, Azzolini O, Banks TI, et al. CUORE sensitivity to $0\nu\beta\beta$ decay. *Eur Phys J C.* (2017) **77**:532. doi: 10.1140/epjc/s10052-017-5098-9
82. Kotila J, Iachello F. Phase space factors for double-β decay. *Phys Rev C* (2012) **85**:034316. doi: 10.1103/PhysRevC.85.034316
83. Barea J, Kotila J, Iachello F. $0\nu\beta\beta$ and $2\nu\beta\beta$ nuclear matrix elements in the interacting boson model with isospin restoration. *Phys Rev C.* (2015) **91**:034304. doi: 10.1103/PhysRevC.91.034304
84. Šimkovic F, Rodin V, Faessler A, Vogel P. $0\nu\beta\beta$ and $2\nu\beta\beta$ nuclear matrix elements, quasiparticle random-phase approximation, and isospin symmetry restoration. *Phys Rev C.* (2013) **87**:045501. doi: 10.1103/PhysRevC.87.045501
85. Vissani F. Signal of neutrinoless double beta decay, neutrino spectrum and oscillation scenarios. *J High Energy Phys.* (1999) **6**:022. doi: 10.1088/1126-6708/1999/06/022
86. Dell'Oro S, Marcocci S, Vissani F. New expectations and uncertainties on neutrinoless double beta decay. *Phys Rev D.* (2014) **90**:033005. doi: 10.1103/PhysRevD.90.033005
87. Capozzi F, Lisi E, Marrone A, Montanino D, Palazzo A. Neutrino masses and mixings: Status of known and unknown 3ν parameters. *Nucl Phys B.* (2016) **908**:218–34. doi: 10.1016/j.nuclphysb.2016.02.016
88. Arnold R, Augier C, Baker J, Barabash AS, Basharina-Freshville A, Blondel S, et al. Result of the search for neutrinoless double-β decay in ^{100}Mo with the NEMO-3 experiment. *Phys Rev D.* (2015) **92**:072011. doi: 10.1103/PhysRevD.92.072011
89. Tomoda T. $0^+ \rightarrow 2^+ 0\nu\beta\beta$ decay triggered directly by the Majorana neutrino mass. *Phys Lett B.* (2000) **474**:245–50. doi: 10.1016/S0370-2693(00)00025-3
90. Šimkovic F, Faessler A. Distinguishing the $0\nu\beta\beta$-decay mechanisms. *Prog Part Nucl Phys.* (2002) **48**:201–9. doi: 10.1016/S0146-6410(02)00125-4
91. Aunola M, Suhonen J. Systematic study of beta and double beta decay to excited final states. *Nucl Phys A.* (1996) **602**:133–66. doi: 10.1016/0375-9474(96)00087-5
92. Suhonen J, Civitarese O. Weak-interaction and nuclear-structure aspects of nuclear double beta decay. *Phys Rep.* (1998) **300**:123–214. doi: 10.1016/S0370-1573(97)00087-2

93. Alduino C, Alfonso K, Artusa DR, Avignone FT, Azzolini O, Banks TI, et al. Double-beta decay of ^{130}Te to the first 0^+ excited state of ^{130}Xe with CUORE−0 (2018). *arXiv [Preprint]. arXiv:1811.10363*.
94. Alessandrello A, Brofferio C, Camin DV, Cremonesi O, Fiorini E, Giuliani A, et al. Preliminary results on double beta decay of ^{130}Te with an array of twenty cryogenic detectors. *Phys Lett B.* (1998) **433**:156–62. doi: 10.1016/S0370-2693(98)00645-5
95. Andreotti E, Arnaboldi C, Avignone FT, Balata M, Bandac I, Barucci M, et al. Search for double-β decay of ^{130}Te to the first 0^+ excited state of ^{130}Xe with the CUORICINO experiment bolometer array. *Phys Rev C.* (2012) **85**:045503.
96. Pozzi S. *Search for double-beta decay of ^{130}Te to the excited states of ^{130}Xe in CUORE-0.* (Ph. D. thesis). Università degli Studi di Milano-Bicocca, Milano, Italy (2017).
97. Wang M, Audi G, Kondev FG, Huang WJ, Naimi S, Xu X. The AME2016 atomic mass evaluation (II). Tables, graphs and references. *Chin Phys C.* (2017) **41**:030003. doi: 10.1088/1674-1137/41/3/030003
98. Vergados JD. Lepton-violating $\beta^-\beta^-$, $\beta^+\beta^+$ decays, (e^-, e^+) conversion and double electron capture in gauge theories. *Nucl Phys B.* (1983) **218**:109–44. doi: 10.1016/0550-3213(83)90477-7
99. Kotila J, Barea J, Iachello F. Neutrinoless double-electron capture. *Phys Rev C.* (2014) **89**:064319. doi: 10.1103/PhysRevC.89.064319
100. Alduino C, Alfonso K, Artusa DR, Avignone FT, Azzolini O, Bari G, et al. Search for neutrinoless β^+EC decay of ^{120}Te with CUORE-0. *Phys Rev C.* (2018) **97**:055502. doi: 10.1103/PhysRevC.97.055502
101. Andreotti E, Arnaboldi C, Avignone FT, Balata M, Bandac I, Barucci M, et al. Search for β^+/ec double beta decay of ^{120}Te. *Astropart Phys.* (2011) **34**:643–8. doi: 10.1016/j.astropartphys.2010.12.011
102. Takaoka N, Motomura Y, Nagao K. Half-life of ^{130}Te double-β decay measured with geologically qualified samples. *Phys Rev C* (1996) **53**:1557. doi: 10.1103/PhysRevC.53.1557
103. Gelmini GB, Roncadelli M. Left-handed neutrino mass scale and spontaneously broken lepton number. *Phys Lett B.* (1981) **99**:411–5. doi: 10.1016/0370-2693(81)90559-1
104. Burgess CP, Cline JM. New class of Majoron−emitting double-β decays. *Phys Rev D.* (1994) **49**:5925–44. doi: 10.1103/PhysRevD.49.5925
105. Bamert P, Burgess CP, Mohapatra RN. Multi-majoron modes for neutrinoless double-beta decay. *Nucl Phys B.* (1995) **449**:25–48. doi: 10.1016/0550-3213(95)00273-U
106. Gando A, Gando Y, Hanakago H, Ikeda H, Inoue K, Kato R, et al. Limits on majoron-emitting double-β decays of ^{136}Xe in the KamLAND−Zen experiment. *Phys Rev C.* (2012) **86**:021601. doi: 10.1103/PhysRevC.86.021601
107. Elliott SR, Hahn AA, Moe MK. Limit on neutrinoless double-beta decay with majoron emission in ^{82}Se. *Phys Rev Lett.* (1987) **59**:1649–51. doi: 10.1103/PhysRevLett.59.1649
108. Arnold R, Augier C, Baker J, Barabash AS, Brudanin V, Caffrey AJ, et al. Limits on different majoron decay modes of ^{100}Mo and ^{82}Se for neutrinoless double beta decays in the NEMO−3 experiment. *Nucl Phys A.* (2006) **765**:483–94. doi: 10.1016/j.nuclphysa.2005.11.015
109. Arnold R, Augier C, Barabash AS, Basharina-Freshville A, S B, Blot S, et al. Detailed studies of ^{100}Mo two-neutrino double beta decay in NEMO-3. *arXiv [Preprint]. arXiv:1903.08084* (2019).
110. Wang G, Chang CL, V Y, Ding J, Novosad V, Bucci C, et al. CUPID: CUORE (cryogenic underground observatory for rare events) upgrade with particle iDentification. *arXiv [Preprint]. arXiv:1504.03599* (2015).
111. Bergé L, Chapellier M, de Combarieu M, Dumoulin L, Giuliani A, Gros M, et al. Complete event-by-event $\alpha/\gamma(\beta)$ separation in a full-size TeO_2 CUORE bolometer by simultaneous heat and light detection. *Phys Rev C.* (2018) **97**:032501. doi: 10.1103/PhysRevC.97.032501
112. Goeppert-Mayer M. Double beta-disintegration. *Phys Rev.* (1935) **48**:512–6. doi: 10.1103/PhysRev.48.512
113. Beeman JW, Danevich FA, Degoda VY, Galashov EN, Giuliani A, Kobychev VV, et al. A next generation neutrinoless double beta decay experiment based on $ZnMoO_4$ scintillating bolometers. *Phys Lett B.* (2012) **710**:318–23. doi: 10.1016/j.physletb.2012.03.009
114. Chernyak DM, Danevich FA, Giuliani A, Olivieri E, Tenconi M, Tretyak VI. Random coincidence of $2\nu2\beta$ decay events as a background source in bolometric $0\nu2\beta$ decay experiments. *Eur Phys J C.* (2012) **72**:1989. doi: 10.1140/epjc/s10052-012-1989-y
115. Artusa DR, Avignone FT, Azzolini O, Balata M, Banks TI, Bari G, et al. Exploring the neutrinoless double beta decay in the inverted neutrino hierarchy with bolometric detectors. *Eur Phys J C.* (2014) **74**:3096. doi: 10.1140/epjc/s10052-014-3096-8
116. Ouellet J. Latest Results from the CUORE Experiment. In: *Proceedings of the International Conference Neutrino-2018.* (2018). doi: 10.5281/zenodo.1286904
117. Voloshin MB, Okun LB. On the electric charge conservation. *JETP Lett.* (1978) **28**:145.
118. Okun LB, Zeldovich YB. Paradoxes of unstable electron. *Phys Lett B.* (1978) **78**:597–600. doi: 10.1016/0370-2693(78)90648-2
119. Ignatiev AY, Kuzmin VA, Shaposhnikov ME. Is the electric charge conserved? *Phys Lett B.* (1979) **84**:315–8. doi: 10.1016/0370-2693(79)90048-0
120. Belli P, Bernabei R, Dai CJ, Ignesti G, Incicchitti A, Montecchia F, et al. Quest for electron decay $e^- \rightarrow \nu_e\gamma$ with a liquid xenon scintillator. *Phys Rev D.* (2000) **61**:117301. doi: 10.1103/PhysRevD.61.117301
121. Agostini M, Appel S, Bellini G, Benziger J, Bick D, Bonfini G, et al. A test of electric charge conservation with Borexino. *Phys Rev Lett.* (2015) **115**:231802. doi: 10.1103/PhysRevLett.115.231802
122. Colladay D, Kostelecký VA. CPT violation and the standard model. *Phys Rev D.* (1997) **55**:6760–74. doi: 10.1103/PhysRevD.55.6760
123. Colladay D, Kostelecký VA. Lorentz-violating extension of the Standard Model. *Phys Rev D.* (1998) **58**:116002. doi: 10.1103/PhysRevD.58.116002
124. Kostelecký VA. Gravity, Lorentz violation, and the Standard Model. *Phys Rev D.* (2004) **69**:105009. doi: 10.1103/PhysRevD.69.105009
125. Diaz JS. Limits on Lorentz and CPT violation from double beta decay. *Phys Rev D.* (2014) **89**:036002. doi: 10.1103/PhysRevD.89.036002
126. Albert JB, Barbeau PS, Beck D, Belov V, Breidenbach M, Brunner T, et al. First Search for Lorentz and CPT Violation in Double Beta Decay with EXO-200. *Phys Rev D.* (2016) **93**:072001. doi: 10.1103/PhysRevD.93.072001
127. Nutini I. *The CUORE experiment: detector optimization and modelling and CPT conservation limit.* (Ph. D. thesis). INFN - Gran Sasso Science Institute, l'Aquila, Italy (2019).
128. Greenberg OW. On the surprising rigidity of the Pauli exclusion principle. *Nucl Phys B Proc Suppl.* (1989) **6**:83–9. doi: 10.1016/0920-5632(89)90405-2
129. Belli P, Bernabei R, Dai CJ, He HL, Ignesti G, Incicchitti A, et al. New experimental limit on the electron stability and non-paulian transitions in Iodine atoms. *Phys Lett B.* (1999) **460**:236–41. doi: 10.1016/S0370-2693(99)00783-2
130. Bellini G, Bonetti S, Buizza Avanzini M, Caccianiga B, D'Angelo D, Franco D, et al. New experimental limits on the Pauli-forbidden transitions in ^{12}C nuclei obtained with 485 days Borexino data. *Phys Rev C.* (2010) **81**:034317. doi: 10.1103/PhysRevC.81.034317
131. Abgrall N, Arnquist FT I J Avignone, Barabash AS, Bertrand FE, Bradley AW, et al. Search for Pauli exclusion principle violating atomic transitions and electron decay with a p-type point contact germanium detector. *Eur Phys J C.* (2016) **76**:619. doi: 10.1140/epjc/s10052-016-4467-0
132. Shi H, Milotti E, Bartalucci S, Bazzi M, Bertolucci S, Bragadireanu AM, et al. Experimental search for the violation of Pauli exclusion principle. *Eur Phys J C.* (2018) **78**:319. doi: 10.1140/epjc/s10052-018-5802-4
133. Elliott SR, LaRoque BH, Gehman VM, Kidd MF, Chen M. An improved limit on pauli-exclusion-principle forbidden atomic transitions. *Found Phys.* (2012) **42**:1015–30. doi: 10.1007/s10701-012-9643-y
134. Babu KS, Gogoladze I, Wang K. Gauged baryon parity and nucleon stability. *Phys Lett B.* (2003) **570**:32–8. doi: 10.1016/j.physletb.2003.07.036
135. Albert JB, Anton G, Badhrees I, Barbeau PS, Bayerlein R, Beck D, et al. Search for nucleon decays with EXO-200. *Phys Rev D.* (2018) **97**:072007. doi: 10.1103/PhysRevD.97.072007
136. Alvis SI, Arnquist IJ, Avignone FT, Barabash AS, Barton CJ, Bertrand FE, et al. Search for tri-nucleon decay in the majorana demonstrator. *arXiv:1812.01090* (2018).
137. Heintze J. On the question of the natural radioactivity of ^{50}V, ^{113}In and ^{123}Te (in German). *Z Naturforsch A.* (1955) **10**:77. doi: 10.1515/zna-1955-0113

138. Alessandrello A, Arnaboldi C, Brofferio C, Capelli S, Cremonesi O, Fiorini E, et al. New limits on naturally occurring electron capture of ^{123}Te. *Phys Rev. C.* (2003) **67**:014323. doi: 10.1103/PhysRevC.67.014323
139. Watt DE, Glover RN. A search for radioactivity among the naturally occurring isobaric pairs. *Philos Mag.* (1962) **7**:105–14. doi: 10.1080/14786436208201861
140. Alessandria F, Ardito R, Artusa DR, Avignone FT, Azzolini O, Balata M, et al. The low energy spectrum of TeO_2 bolometers: results and dark matter perspectives for the CUORE-0 and CUORE experiments. *J Cosm Astropart Phys.* (2013) **1**:038. doi: 10.1088/1475-7516/2013/01/038
141. Pedretti M. *The single module for Cuoricino and CUORE detectors: tests, construction and modeling*. (Ph. D. thesis). Università dell'Insubria, Como, Italy (2004).
142. Vignati M. *Model of the response function of CUORE bolometers.* (Ph. D. thesis). Università di Roma-La Sapienza (2010).
143. Santone D. *Pulse shape analysis of CUORE-0 bolometers for a better comprehension of detector response*. (Ph. D. thesis). Università dell'Aquila, l'Aquila, Italy (2017).
144. Casali N, Vignati M, Beeman JW, Bellini F, Cardani L, Dafinei I, et al. TeO_2 bolometers with Čerenkov signal tagging: towards next-generation neutrinoless double beta decay experiments. *Eur Phys J C.* (2015) **75**:12. doi: 10.1140/epjc/s10052-014-3225-4
145. Kim GB, Choi S, Danevich FA, Fleischmann A, Kang CS, Kim HJ, et al. A $CaMoO_4$ crystal low temperature detector for the AMoRE neutrinoless double beta decay search. *Adv High Energy Phys.* (2015) **2015**:817530. doi: 10.1155/2015/817530
146. Artusa DR, Balzoni A, Beeman JW, Bellini F, Biassoni M, Brofferio C, et al. First array of enriched $Zn^{82}Se$ bolometers to search for double beta decay. *Eur Phys J C.* (2016) **76**:364. doi: 10.1140/epjc/s10052-016-4223-5
147. Tabarelli de Fatis T. Cerenkov emission as a positive tag of double beta decays in bolometric experiments. *Eur Phys J C.* (2010) **65**:359–61. doi: 10.1140/epjc/s10052-009-1207-8
148. Schäffner K, Angloher G, Bellini F, Casali N, Ferroni F, Hauff D, et al. Particle discrimination in TeO_2 bolometers using light detectors read out by transition edge sensors. *Astropart Phys.* (2015) **69**:30–6. doi: 10.1016/j.astropartphys.2015.03.008
149. Willers M, Feilitzsch FV, Gutlein A, Munster A, Lanfranchi JC, Oberauer L, et al. Neganov-Luke amplified cryogenic light detectors for the background discrimination in neutrinoless double beta decay search with TeO_2 bolometers. *J Instrum.* (2015) **10**:P03003. doi: 10.1088/1748-0221/10/03/P03003
150. Battistelli ES, Bellini F, Bucci C, Calvo M, Cardani L, Casali N, et al. CALDER: neutrinoless double-beta decay identification in TeO_2 bolometers with kinetic inductance detectors. *Eur Phys J C.* (2015) **75**:353. doi: 10.1140/epjc/s10052-015-3575-6
151. Bellini F, Cardani L, Casali N, Colantoni I, Cruciani A, Bellini F, Castellano MG, et al. High sensitivity phonon-mediated kinetic inductance detector with combined amplitude and phase read-out. *Appl Phys Lett.* (2017) **110**:033504. doi: 10.1063/1.4974082
152. Pattavina L, Casali N, Dumoulin L, Giuliani A, Mancuso M, de Marcillac P, et al. Background suppression in massive TeO_2 bolometers with Neganov' Luke amplified light detectors. *J Low Temp Phys.* (2016) **184**:286–91. doi: 10.1007/s10909-015-1404-9
153. Biassoni M, Brofferio C, Capelli S, Cassina L, Clemenza M, Cremonesi O, et al. Large area Si low-temperature light detectors with Neganov' Luke effect. *Eur Phys J C.* (2015) **75**:480. doi: 10.1140/epjc/s10052-015-3712-2
154. Nones C, Bergé L, Dumoulin L, Marnieros S, Olivieri E. Superconducting aluminum layers as pulse shape modifiers: an innovative solution to fight against surface background in neutrinoless double beta decay experiments. *J Low Temp Phys.* (2012) **167**:1029–34. doi: 10.1007/s10909-012-0558-y
155. Canonica L, Biassoni M, Brofferio C, Bucci C, Calvano S, Di Vacri ML, et al. Rejection of surface background in thermal detectors: the ABSuRD project. *Nucl Instrum Meth A.* (2013) **732**:286–9. doi: 10.1016/j.nima.2013.05.114
156. Wang G, Chang CL, Yefremenko V, Ding J, Novosad V, Bucci C, et al. R&D towards CUPID (CUORE upgrade with particle iDentification). *arXiv [Preprint]. arXiv:1504.03612* (2015).

Conflict of Interest Statement: The authors declare that the research was conducted in the absence of any commercial or financial relationships that could be construed as a potential conflict of interest.